

FIG. 6. AM demethylation activity of CYP2B6 proteins expressed in COS-7 cells. The concentration of AM was 50 μ M. Each number corresponds to CYP2B6 variant proteins. Results are presented as the mean \pm S.D. in triplicate. *, $P < 0.05$ compared with CYP2B6.1. N.D., not detectable.

has the highest intrinsic activity for AM demethylation, followed by CYP3A4. In the kinetic parameter analysis, the affinity of CYP2B6 was 4-fold higher than that of CYP3A4, and the $V_{max}/$ apparent K_m of CYP2B6 was 6-fold higher than that of CYP3A4. These results suggest that AM demethylation is likely to be mainly catalyzed by CYP2B6 in the liver. The contribution of CYP2B6 to AM demethylation by human liver microsomes was further substantiated by showing a correlation to CYP2B6 protein content ($r^2 = 0.548$). However, van Agtmael et al. (1999b,c) have reported that administration of AM with grapefruit juice, a CYP3A4 inhibitor, increased the blood concentration of AM and DHA but not their elimination half-life. Thus, CYP3A4 in the small intestine might also play an important role in the metabolism of AM.

CYP2B6 is a genetically polymorphic enzyme (Zanger et al., 2007; Arenaz et al., 2010). In vitro functional characterization of polymorphically expressed CYP2B6 variants revealed that CYP2B6.4 and CYP2B6.6 increased AM demethylation activity, whereas CYP2B6.8, CYP2B6.11, CYP2B6.12, CYP2B6.14, CYP2B6.15, CYP2B6.16, CYP2B6.18, CYP2B6.20, CYP2B6.21, CYP2B6.24, and CYP2B6.27 exhibited no activity or decreased activity. These alterations were consistent with those of previous in vitro studies performed using bupropion, 7-ethoxy-4-trifluoromethylcoumarin, and selegiline as CYP2B6 substrates (Lang et al., 2004; Klein et al., 2005; Wang et al., 2006; Rotger et al., 2007; Watanabe et al., 2010). However, CYP2B6.2 exhibited increased AM demethylation activity, and the activity of CYP2B6.13 was similar to that of wild-type CYP2B6.1. There have been several reports that CYP2B6.2 exhibited no functional differences compared with CYP2B6.1 (Jinno et al., 2003;

Watanabe et al., 2010) and that CYP2B6.13 had no metabolic activity toward 7-ethoxy-4-trifluoromethylcoumarin and selegiline (Watanabe et al., 2010). These results suggest that these CYP2B6 variants show substrate-dependent changes in the catalytic properties of the enzyme.

Gay et al. (2010) recently determined the crystal structure of CYP2B6, allowing the prediction of precise locations within the three-dimensional structure at which amino acid substitutions occur. They suggested that the K262R substitution on the G/H loop is assembled into a hydrogen-bonding network with His252, Thr255, Asp263, and Asp266 and is involved in protein stability. In this study, the AM demethylation activities of CYP2B6.12 (G99E) and CYP2B6.24 (Q476D) were not detectable. In the CYP2B6 protein structure, the Gly99 and Gln476 residues are located in substrate recognition site 1 and 6, respectively. These amino acid changes may reduce the affinity of CYP2B6 for AM. However, a number of amino acids with altered AM demethylation activity are located far from substrate recognition sites. Indeed, the apparent K_m values of AM demethylation were not significantly different among the CYP2B6 variants (Table 1). We hypothesize that the functional effects of these variants are transduced via long-range hydrogen-bonding networks or through subtle differences in the placement of secondary structural elements. In addition, most of the amino acid substitutions that abolished enzymatic activity are conserved among human P450s and are therefore critical for CYP2B6 activity.

This is the first study to functionally analyze CYP2B6 genetic variants with respect to AM demethylation activity. If CYP2B6 has a significant role in the metabolism of AM in vivo as well as in vitro, individuals with poor CYP2B6 metabolism might have higher plasma

TABLE 1

Kinetic parameters of AM demethylation by CYP2B6 proteins expressed in COS-7 cells

Results represent the mean \pm S.D. of triplicate determinations.

Variants	Apparent K_m μ M	V_{max} $\text{pmol} \cdot \text{min}^{-1} \cdot \text{pmol CYP2B6}^{-1}$	$V_{max}/$ Apparent K_m $\mu\text{l} \cdot \text{min}^{-1} \cdot \text{pmol CYP2B6}^{-1}$	$V_{max}/$ Apparent K_m Ratio % CYP2B6.1
CYP2B6.1	3.10 \pm 1.1	36.0 \pm 5.67	12.4 \pm 4.11	
CYP2B6.2	4.29 \pm 2.7	64.4 \pm 3.92*	18.8 \pm 9.19	129
CYP2B6.4	2.73 \pm 0.45	70.6 \pm 9.29*	26.0 \pm 2.42	223
CYP2B6.5	6.87 \pm 6.8	19.8 \pm 3.06	8.91 \pm 11.3	24.8
CYP2B6.6	6.72 \pm 3.0	150 \pm 15.9*	24.2 \pm 6.84	192
CYP2B6.7	2.80 \pm 1.4	50.1 \pm 12.3	19.2 \pm 4.65	154
CYP2B6.9	4.44 \pm 1.7	33.1 \pm 5.20	8.38 \pm 3.94	64.2
CYP2B6.10	1.93 \pm 0.68	17.0 \pm 5.03	9.98 \pm 5.05	75.7
CYP2B6.13	7.33 \pm 4.1	18.2 \pm 5.54	2.93 \pm 1.73	21.3
CYP2B6.14	5.06 \pm 5.8	7.06 \pm 1.63*	6.70 \pm 9.40	12.0
CYP2B6.17	2.17 \pm 0.40	21.2 \pm 4.73	9.44 \pm 2.45	84.0
CYP2B6.19	8.06 \pm 8.9	36.9 \pm 21.9	7.38 \pm 6.15	39.4
CYP2B6.20	6.47 \pm 9.8	9.85 \pm 2.22*	8.79 \pm 7.22	13.1
CYP2B6.23	1.91 \pm 0.72	31.4 \pm 7.71	17.6 \pm 5.93	142
CYP2B6.25	2.04 \pm 1.9	25.7 \pm 7.31	21.6 \pm 15.7	108
CYP2B6.26	5.50 \pm 3.4	37.3 \pm 6.04	10.1 \pm 8.13	58.4
CYP2B6.27	4.50 \pm 0.98	10.6 \pm 6.16*	2.59 \pm 1.82	20.2

* $P < 0.05$ compared with CYP2B6.1.

AM concentrations than those with more active variants of this enzyme. However, because DHA also has an antimalarial effect, it would be difficult to assess the clinical outcome in subjects who polymorphically express CYP2B6 without *in vivo* data. To more fully understand the mechanistic basis of our findings, it would be of great value to clinically examine the relationship between CYP2B6 genotypes and the plasma concentration of AM and its metabolites.

In conclusion, demethylation of AM was mainly catalyzed by recombinant CYP2B6, although recombinant CYP3A4 also exhibited this metabolic activity. In addition, we performed a comprehensive analysis, using COS-7 cells as a heterologous expression system, to characterize nonsynonymous CYP2B6 variants. Many of the 26 variants expressed in COS-7 cells exhibited significantly altered AM demethylation activity. This study provides insights into the genotype-phenotype associations of CYP2B6 and lays a foundation for future clinical studies on interindividual variation in drug efficacy and toxicity.

Authorship Contributions

Participated in research design: Honda, Hirasawa, and Hiratsuka.

Conducted experiments: Honda, Muroi, and Tamaki.

Contributed new reagents or analytic tools: Saigusa, Suzuki, Tomioka, and Matsubara.

Performed data analysis: Honda, Oda, and Hiratsuka.

Wrote or contributed to the writing of the manuscript: Honda, Saigusa, and Hiratsuka.

References

- Ali S, Najmi MH, Tarning J, and Lindegardh N (2010) Pharmacokinetics of artemether and dihydroartemisinin in healthy Pakistani male volunteers treated with artemether-lumefantrine. *Malar J* 9:275.
- Arenaz I, Vicente J, Fanlo A, Vázquez P, Medina JC, Conde B, González-Andrade F, and Sinués B (2010) Haplotype structure and allele frequencies of CYP2B6 in Spaniards and Central Americans. *Fundam Clin Pharmacol* 24:247–253.
- Asimus S and Ashton M (2009) Artemisinin—a possible CYP2B6 probe substrate? *Biopharm Drug Dispos* 30:265–275.
- Brewer TG, Grate SJ, Peggins JO, Weina PJ, Petras JM, Levine BS, Heiffer MH, and Schuster BG (1994) Fatal neurotoxicity of arteether and artemether. *Am J Trop Med Hyg* 51:251–259.
- Gautam A, Ahmed T, Batra V, and Paliwal J (2009) Pharmacokinetics and pharmacodynamics of endoperoxide antimalarials. *Curr Drug Metab* 10:289–306.
- Gay SC, Shah MB, Talakad JC, Maekawa K, Roberts AG, Wilderman PR, Sun L, Yang JY, Huelga SC, Hong WX, et al. (2010) Crystal structure of a cytochrome P450 2B6 genetic variant in complex with the inhibitor 4-(4-chlorophenyl)imidazole at 2.0-Å resolution. *Mol Pharmacol* 77:529–538.
- Hesse LM, Venkatakrishnan K, Court MH, von Moltke LL, Duan SX, Shader RI, and Greenblatt DJ (2000) CYP2B6 mediates the *in vitro* hydroxylation of bupropion: potential drug interactions with other antidepressants. *Drug Metab Dispos* 28:1176–1183.
- Hidestrand M, Oscarson M, Salonen JS, Nyman L, Pelkonen O, Turpeinen M, and Ingelman-Sundberg M (2001) CYP2B6 and CYP2C19 as the major enzymes responsible for the metabolism of selegiline, a drug used in the treatment of Parkinson's disease, as revealed from experiments with recombinant enzymes. *Drug Metab Dispos* 29:1480–1484.
- Hien TT and White NJ (1993) Qinghaosu. *Lancet* 341:603–608.
- Human Cytochrome P450 (CYP) Allele Nomenclature Committee (2008) CYP2B6 nomenclature. Available at: <http://www.cypalleles.ki.se/cyp2b6.htm>.
- Huang L, Jayewardene AL, Li X, Marzan F, Lizak PS, and Aweeka FT (2009) Development and validation of a high-performance liquid chromatography/tandem mass spectrometry method for the determination of artemether and its active metabolite dihydroartemisinin in human plasma. *J Pharm Biomed Anal* 50:959–965.
- Jinno H, Tanaka-Kagawa T, Ohno A, Makino Y, Matsushima E, Hanioka N, and Ando M (2003) Functional characterization of cytochrome P450 2B6 allelic variants. *Drug Metab Dispos* 31:398–403.
- Klayman DL (1985) Qinghaosu (artemisinin): an antimalarial drug from China. *Science* 228:1049–1055.
- Klein K, Lang T, Saussele T, Barbosa-Sicard E, Schunck WH, Eichelbaum M, Schwab M, and Zanger UM (2005) Genetic variability of CYP2B6 in populations of African and Asian origin: allele frequencies, novel functional variants, and possible implications for anti-HIV therapy with efavirenz. *Pharmacogenet Genomics* 15:861–873.
- Lang T, Klein K, Richter T, Zibat A, Kerb R, Eichelbaum M, Schwab M, and Zanger UM (2004) Multiple novel nonsynonymous CYP2B6 gene polymorphisms in Caucasians: demonstration of phenotypic null alleles. *J Pharmacol Exp Ther* 311:34–43.
- Le Bras J and Durand R (2003) The mechanisms of resistance to antimalarial drugs in *Plasmodium falciparum*. *Fundam Clin Pharmacol* 17:147–153.
- Lefèvre G, Carpenter P, Souppart C, Schmidli H, McClean M, and Stypinski D (2002) Pharmacokinetics and electrocardiographic pharmacodynamics of artemether-lumefantrine (Riamet) with concomitant administration of ketoconazole in healthy subjects. *Br J Clin Pharmacol* 54:485–492.
- Mo SL, Liu YH, Duan W, Wei MQ, Kanwar JR, and Zhou SF (2009) Substrate specificity, regulation, and polymorphism of human cytochrome P450 2B6. *Curr Drug Metab* 10:730–753.
- Mordí MN, Mansor SM, Navaratnam V, and Wernsdorfer WH (1997) Single dose pharmacokinetics of oral artemether in healthy Malaysian volunteers. *Br J Clin Pharmacol* 43:363–365.
- Mwesigwa J, Parikh S, McGee B, German P, Drysdale T, Kalyango JN, Clark TD, Dorsey G, Lindegardh N, Annerberg A, et al. (2010) Pharmacokinetics of artemether-lumefantrine and artesunate-amodiaquine in children in Kampala, Uganda. *Antimicrob Agents Chemother* 54:52–59.
- Na Bangchang K, Karbwang J, Thomas CG, Thanavibul A, Sukontason K, Ward SA, and Edwards G (1994) Pharmacokinetics of artemether after oral administration to healthy Thai males and patients with acute, uncomplicated falciparum malaria. *Br J Clin Pharmacol* 37:249–253.
- Nakajima M, Komagata S, Fujiki Y, Kanada Y, Ebi H, Itoh K, Mukai H, Yokoi T, and Minami H (2007) Genetic polymorphisms of CYP2B6 affect the pharmacokinetics/pharmacodynamics of cyclophosphamide in Japanese cancer patients. *Pharmacogenet Genomics* 17:431–445.
- Navaratnam V, Mansor SM, Sit NW, Grace J, Li Q, and Olliaro P (2000) Pharmacokinetics of artemisinin-type compounds. *Clin Pharmacokinet* 39:255–270.
- Price RN and Nosten F (2001) Drug resistant falciparum malaria: clinical consequences and strategies for prevention. *Drug Resist Updat* 4:187–196.
- Rogier M, Tegude H, Colombo S, Cavassini M, Furrer H, Dècoster L, Blievernicht J, Saussele T, Günthard HF, Schwab M, et al. (2007) Predictive value of known and novel alleles of CYP2B6 for efavirenz plasma concentrations in HIV-infected individuals. *Clin Pharmacol Ther* 81:557–566.
- Roy P, Yu LJ, Crespi CL, and Waxman DJ (1999) Development of a substrate-activity based approach to identify the major human liver P-450 catalysts of cyclophosphamide and ifosfamide activation based on cDNA-expressed activities and liver microsomal P-450 profiles. *Drug Metab Dispos* 27:655–666.
- Salonen JS, Nyman L, Boobis AR, Edwards RJ, Watts P, Lake BG, Price RJ, Renwick AB, Gómez-Lechón MJ, Castell JV, et al. (2003) Comparative studies on the cytochrome p450-associated metabolism and interaction potential of selegiline between human liver-derived *in vitro* systems. *Drug Metab Dispos* 31:1093–1102.
- van Agtmael MA, Cheng-Qi S, Qing JX, Mull R, and van Boxtel CJ (1999a) Multiple dose pharmacokinetics of artemether in Chinese patients with uncomplicated falciparum malaria. *Int J Antimicrob Agents* 12:151–158.
- van Agtmael MA, Gupta V, van der Graaf CA, and van Boxtel CJ (1999b) The effect of grapefruit juice on the time-dependent decline of artemether plasma levels in healthy subjects. *Clin Pharmacol Ther* 66:408–414.
- van Agtmael MA, Gupta V, van der Wösten TH, Rutten JP, and van Boxtel CJ (1999c) Grapefruit juice increases the bioavailability of artemether. *Eur J Clin Pharmacol* 55:405–410.
- van Agtmael MA, Van Der Graaf CA, Dien TK, Koopmans RP, and van Boxtel CJ (1998) The contribution of the enzymes CYP2D6 and CYP2C19 in the demethylation of artemether in healthy subjects. *Eur J Drug Metab Pharmacokinet* 23:429–436.
- Wang J, Sönnnerborg A, Rane A, Josephson F, Lundgren S, Ståhle L, and Ingelman-Sundberg M (2006) Identification of a novel specific CYP2B6 allele in Africans causing impaired metabolism of the HIV drug efavirenz. *Pharmacogenet Genomics* 16:191–198.
- Watanabe T, Sakuyama K, Sasaki T, Ishii Y, Ishikawa M, Hirasawa N, and Hiratsuka M (2010) Functional characterization of 26 CYP2B6 allelic variants (CYP2B6.2-CYP2B6.28, except CYP2B6.22). *Pharmacogenet Genomics* 20:459–462.
- Wernsdorfer WH (1991) The development and spread of drug-resistant malaria. *Parasitol Today* 7:297–303.
- Woodrow CJ, Haynes RK, and Krishna S (2005) *Artemisinins Postgrad Med J* 81:71–78.
- World Health Organization (2010) *Guidelines for Treatment of Malaria*, 2nd ed., World Health Organization, Geneva, Switzerland. Available from http://whqlibdoc.who.int/publications/2010/9789241547925_eng.pdf.
- Xie H, Griskevicius L, Ståhle L, Hassan Z, Yasar U, Rane A, Broberg U, Kimby E, and Hassan M (2006) Pharmacogenetics of cyclophosphamide in patients with hematological malignancies. *Eur J Pharm Sci* 27:54–61.
- Xie HJ, Yasar U, Lundgren S, Griskevicius L, Terelius Y, Hassan M, and Rane A (2003) Role of polymorphic human CYP2B6 in cyclophosphamide bioactivation. *Pharmacogenomics J* 3:53–61.
- Zanger UM, Klein K, Saussele T, Blievernicht J, Hofmann MH, and Schwab M (2007) Polymorphic CYP2B6: molecular mechanisms and emerging clinical significance. *Pharmacogenomics* 8:743–759.

Address correspondence to: Dr. Masahiro Hiratsuka, Laboratory of Pharmacotherapy of Life-Style Related Diseases, Graduate School of Pharmaceutical Sciences, Tohoku University, Sendai, Japan, 6-3, Aoba, Aramaki, Aoba-ku, Sendai 980-8578, Japan. E-mail: mhira@m.tohoku.ac.jp

SNP Communication

Novel Single Nucleotide Polymorphism of
the CYP2A13 Gene in Japanese IndividualsYuichiro TAMAKI¹, Masashi HONDA¹, Yuka MUROI¹, Tomio ARAI², Haruhiko SUGIMURA³, Yoichi MATSUBARA⁴,
Shuichi KANNO⁵, Masaaki ISHIKAWA⁵, Noriyasu HIRASAWA¹ and Masahiro HIRATSUKA^{1,*}¹Laboratory of Pharmacotherapy of Life-Style Related Diseases, Graduate School of Pharmaceutical Sciences,
Tohoku University, Sendai, Japan²Department of Pathology, Tokyo Metropolitan Geriatric Hospital, Tokyo, Japan³Department of Pathology I, Hamamatsu University School of Medicine, Hamamatsu, Japan⁴Department of Medical Genetics, Tohoku University School of Medicine, Sendai, Japan⁵Department of Clinical Pharmacotherapeutics, Tohoku Pharmaceutical University, Sendai, JapanFull text of this paper is available at <http://www.jstage.jst.go.jp/browse/dmpk>

Summary: Cytochrome P450 2A13 (CYP2A13) is a human CYP enzyme that is selectively expressed in the respiratory tract. It plays an active role in the metabolic activation of a tobacco-specific procarcinogen. In this study, the entire coding sequence and the exon-intron junctions of the CYP2A13 gene obtained from 395 Japanese individuals were screened for genetic polymorphisms. Eight genetic polymorphisms were found, of which seven gave rise to known variant alleles: CYP2A13*2, CYP2A13*3, CYP2A13*4, CYP2A13*6, and CYP2A13*7. We identified a novel single nucleotide polymorphism (SNP), 5792T>C, in exon 7 that caused an amino acid substitution (Ile331Thr). One of the 395 individuals included in the study was heterozygous for the variant allele, and therefore, the frequency of the allele in the study population was 0.13%.

Keywords: CYP2A13; genetic polymorphism; SNP; Japanese

Introduction

Cytochrome P450s (CYPs) play an important role in the metabolism of a variety of compounds, including therapeutic agents, environmental toxicants, and chemical carcinogens. CYP2A13 is selectively expressed in the human respiratory tract; the highest level of expression is observed in the nasal mucosa, followed by the tracheal mucosa, and finally the lungs.^{1–5} CYP2A13 plays an active role in the metabolism of many xenobiotic compounds such as 4-(methylnitrosamino)-1-(3-pyridyl)-1-butanone (NNK), which is a major tobacco-specific procarcinogen, and *N*-nitrosomethylphenylamine and is also involved in the detoxification of carcinogens including *N,N*-dimethylaniline.³ Therefore, CYP2A13 may play an

important role in xenobiotic toxicity and tobacco-related carcinogenesis in the respiratory tract and lungs.

The CYP2A13 gene is located in a CYP gene cluster on chromosome 19.⁶ To date, nine alleles of CYP2A13 have been identified (CYP2A13*1–9).^{7–9} Genetic variations affecting CYP2A13 enzyme function may lead to interindividual variability in susceptibility to diseases, including lung cancer. In the present study, we screened nine exons and exon-intron junctions of the CYP2A13 gene from 395 Japanese individuals for genetic polymorphisms by using denaturing high-performance liquid chromatography (DHPLC). We identified one novel single nucleotide polymorphism (SNP) of the CYP2A13 gene among the Japanese individuals included in the study; this novel polymorphism was nonsynonymous.

Received; April 17, 2011, Accepted; May 7, 2011

J-STAGE Advance Published Date: May 24, 2011, doi:10.2133/dmpk.DMPK-11-SC-033

*To whom correspondence should be addressed: Masahiro HIRATSUKA, Ph.D., Laboratory of Pharmacotherapy of Life-Style Related Diseases, Graduate School of Pharmaceutical Sciences, Tohoku University, 6-3 Aoba, Aramaki, Aoba-ku, Sendai 980-8578, Japan. Tel. +81-22-717-7049, Fax. +81-22-717-7049, E-mail: mhira@m.tohoku.ac.jp

On March 7, 2011, the variation was not found in the Japanese Single Nucleotide Polymorphism (JSNP) (<http://snp.ims.u-tokyo.ac.jp/>) database, the National Center for Biotechnology Information (<http://www.ncbi.nlm.nih.gov/SNP/>), the Human CYP Allele Nomenclature Committee (<http://www.cypalleles.ki.se/>) database, or the PharmGKB (<http://www.pharmgkb.org/>) database. The CYP2A13 haplotype with 74G>A, 3375C>T, and 5792T>C was assigned as CYP2A13*10 by the Human CYP Allele Nomenclature Committee.

This work was supported by a grant from the Smoking Research Foundation and in part by KAKENHI (20590154) from the Japan Society for the Promotion of Science (JSPS).

Table 1. Amplification and DHPLC conditions for *CYP2A13* SNP analysis of genomic DNA

Exon	Size (bp)	Forward primer (5'-3')	Reverse primer (5'-3')	Annealing temp. (°C)	PCR cycles	DHPLC temp. (°C)
1-5 ¹	4,817	GCTACACTCCACCTCCAGAACTCCAC	AGGTGTGTCTGCTAACCCAGGACATGAACGG	68	25	—
1 ²	257	AACCACCCAGCCATCACCA	CCCACCCCGTGCCACCC	60	25	60.8, 62.8
2 ²	244	GGGGGCTGCTCCCTCTAACCA	ATCCACCTGGCCACCTTCCC	60	25	61.2, 64.2
3 ²	236	CGCCCCCTGACCTCTCTCCA	AGAAAGCGCGGGTCCCG	60	25	64.0
4 ²	241	TGACTCTCTCCCAACCCCTTC	GTTGTGGTAGGGCGCTCACTGG	60	25	61.6, 62.6
5 ²	260	TGACAGCTGCTCTCCCTTCCCA	CCTGGCTTGCACCTGCCTG	60	25	59.7, 61.7
6-9 ¹	3,528	CCCTAGCTCAAACCCTGGTCTCTCTGAGCC	TTCCTCTCATCACAGCTCCTGAAGGACATC	65	25	—
6 ²	230	AAGAGCATGGAGAGTGAGCTTGGTCT	GAGGGTCTGGGGCCCTCACTT	60	25	60.3, 62.3
7 ²	286	CATCCTGTCTAAGACCCCTAGACAC	GAAGTCCCCGTAGTCTGAGTGGTGG	60	25	58.5, 60.5
8 ²	224	CCCCAACCTGCCTCATTACACA	TGTGAGCCGTGGCCTGGC	60	25	59.4, 60.4
9 ²	271	GAGAGTGGGCTTACCTCACCC	GTTCCCTGGCCCCGCC	60	25	59.8, 61.8, 63.8

¹First-round PCR. ²Second-round PCR.

Materials and Methods

Human DNA samples: In the present study, DNA samples were obtained at the autopsies of 395 diseased patients in the Department of Pathology, Tokyo Metropolitan Geriatric Hospital, Tokyo, Japan, and were analyzed. The research protocols were approved by the Ethics Committees of the Tokyo Metropolitan Geriatric Hospital and the Graduate School of Pharmaceutical Sciences, Tohoku University.

Polymerase chain reaction (PCR) and DHPLC conditions: The primer pairs used to amplify the nine exons and the exon-intron junctions of the *CYP2A13* gene are listed in Table 1. These primers were designed on the basis of a genomic sequence reported in GenBank (NG_000008.7). The first-round long PCR was performed to specifically amplify exons 1-5 and 6-9 of the *CYP2A13* gene. Genomic DNA (10-50 ng) was amplified using LA-Taq DNA polymerase (TaKaRa, Otsu, Japan). The PCR thermal profile consisted of an initial denaturation at 95°C for 1 min; followed by 25 repetitive cycles of denaturation at 95°C for 15 s, annealing at 68°C or 65°C for 20 s, and extension at 72°C for 5 min; and then a final extension at 72°C for 7 min.

The first-round PCR products were diluted 1:500 in water and used as DNA templates for the second round of PCR for amplification of all the *CYP2A13* exons. The amplicons for each exon were generated using AmpliTaq Gold PCR Master Mix (Applied Biosystems, Foster City, CA, USA). PCR for the second round comprised an initial denaturation at 95°C for 10 min; followed by 25 repetitive cycles of denaturation at 95°C for 30 s, annealing at 60°C for 30 s, and extension at 72°C for 30 s; and then a final extension at 72°C for 7 min. Heteroduplexes were generated by thermal cycling under the following conditions: 95°C for 1 min, followed by 45 temperature decrements of 1.5°C/min.

The PCR products were analyzed using the DHPLC system WAVE (Transgenomic Inc., Omaha, NE, USA). Amplified PCR samples (5 µL) were separated on a heated C18 reverse-phase column by using 0.1 M triethylammonium acetate (TEAA) in water and 0.1 M TEAA in 25% acetonitrile at a flow rate of 0.9 mL/min. We determined the temperature for heteroduplex separation of a heterozygous *CYP2A13* fragment using the software that was provided with the DHPLC system. The DHPLC running conditions for each amplicon are summarized in Table 1. The linear acetonitrile gradient was adjusted so that the retention time of the DNA peak was 3-5 min. The resultant chromatograms were compared with those of the wild-type DNA. We sequenced both strands of samples in which variants were detected using DHPLC.

To determine the linkage among the polymorphisms identified in this study, we amplified long fragments of DNA obtained from the individuals who were heterozygous for both the SNPs by using PCR. The fragments were run on gels, purified using columns, and then ligated to a pCR-XL-TOPO vector (Invitrogen Co., CA, USA). The ligation products was transfected into *Escherichia coli*, and single colonies (each containing a plasmid with only one of the two alleles) were collected and the plasmids were isolated, after which the plasmid DNA was sequenced.

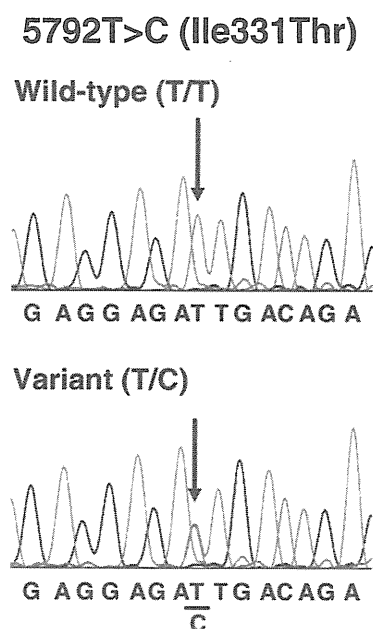
Results and Discussion

We found a novel SNP during this study and provide its details below. SNP: 110224Hiratsuka013; GENE NAME: *CYP2A13*; ACCESSION NUMBER: NG_000008; LENGTH: 25 bases; SEQUENCE: 5'-TCCATGAGGAGAT/CTGACAGAGTGAT-3'.

DHPLC analysis showed that exons 1, 2, 3, 5, 7, and 9 in the *CYP2A13* gene obtained from the 395 DNA samples had distinct chromatographic profiles from those of the wild-type DNA. We tested the specificity of DHPLC for detecting the variant allele in these exons by comparing the

Table 2. Detected SNPs of the CYP2A13 gene in DNA samples of 395 Japanese individuals

Nucleotide change	Location	Predicted amino acid change	Frequency (%)
74G>A	Exon 1	R25Q	5.57
578C>T	Exon 2	R101X	0.38
579G>A	Exon 2	R101Q	0.13
1634_1635insACC	Exon 3	133_134insT	1.77
1706C>G	Exon 3	D158E	1.77
3375C>T	Exon 5	R257C	5.57
5792T>C	Exon 7	I331T	0.13
7465C>T	Exon 9	R494C	0.25

**Fig. 1. Nucleotide sequences of the CYP2A13 gene in exon 7** Although the sequences of only the sense strands are shown here, both strands were sequenced. Arrows indicate the variant nucleotide positions.

results of DHPLC with those of direct sequencing. Eight SNPs (74G>A, 578C>T, 579G>A, 1634_1635insACC, 1706C>G, 3375C>T, 5792T>C, and 7465C>T), including one novel SNP, were detected in the DNA samples of the Japanese individuals included in the study (Table 2). The novel SNP was 5792T>C in exon 7 (Fig. 1), and it resulted in an amino acid change of Ile331Thr. Experimental haplotype analysis by long PCR, cloning, and DNA sequencing showed that three SNPs, 74G>A, 3375C>T, and 5792T>C, exist in the same allele of the CYP2A13 gene (data not shown). One of the 395 individuals was heterozygous for the novel SNP, and therefore, the frequency of the allele in the study population was 0.13%. The allele carrying the 74G>A, 3375C>T, and 5792T>C

SNPs has been designated CYP2A13*10. The allele frequencies of CYP2A13*1 (wild type), *2 (74G>A and 3375C>T), *3 (1634_1635insACC and 1706C>G), *4 (579G>A), *5 (7343T>A), *6 (7465C>T), *7 (578C>T), *8 (1706C>G), and *9 (5294G>T) were 0.916, 0.054, 0.018, 0.001, 0.000, 0.003, 0.004, 0.000, and 0.000, respectively. The sequence of each sample was confirmed by conducting at least two different PCR amplifications.

The novel SNP 5792T>C is located in exon 7 of the CYP2A13 gene and results in an amino acid substitution, Ile331Thr. Smith *et al.* determined the crystalline structure of CYP2A13,¹⁰ thus making it possible to predict precise locations of amino acid substitution within the three-dimensional structure. Ile331 is located at the start of the J-helix of CYP2A13.¹¹ Although this amino acid residue is not located on substrate recognition sites, it is known to be highly conserved in the CYP2 family in mammals. Therefore, the Ile331Thr substitution is expected to alter the catalytic properties of CYP2A13. Further studies are required to elucidate the functional characteristics of the novel variant allele of the CYP2A13 gene.

In conclusion, we identified a novel nonsynonymous SNP in the CYP2A13 gene in Japanese individuals. This nonsynonymous SNP was 5792T>C in exon 7, and it resulted in an amino acid substitution, Ile331Thr. In addition, the allele containing the 74G>A, 3375C>T, and 5792T>C SNPs has been designated CYP2A13*10.

References

- 1) Koskela, S., Hakkola, J., Hukkanen, J., Pelkonen, O., Sorri, M., Saranen, A., Anttila, S., Fernandez-Salguero, P., Gonzalez, F. and Raunio, H.: Expression of CYP2A genes in human liver and extrahepatic tissues. *Biochem. Pharmacol.*, 57: 1407–1413 (1999).
- 2) Gu, J., Su, T., Chen, Y., Zhang, Q. Y. and Ding, X.: Expression of biotransformation enzymes in human fetal olfactory mucosa: potential roles in developmental toxicity. *Toxicol. Appl. Pharmacol.*, 165: 158–162 (2000).
- 3) Su, T., Bao, Z., Zhang, Q. Y., Smith, T. J., Hong, J. Y. and Ding, X.: Human cytochrome P450 CYP2A13: predominant expression in the respiratory tract and its high-efficiency metabolic activation of a tobacco-specific carcinogen, 4-(methylnitrosamino)-1-(3-pyridyl)-1-butanone. *Cancer Res.*, 60: 5074–5079 (2000).
- 4) Chen, Y., Liu, Y. Q., Su, T., Ren, X., Shi, L., Liu, D., Gu, J., Zhang, Q. Y. and Ding, X.: Immunoblot analysis and immunohistochemical characterization of CYP2A expression in human olfactory mucosa. *Biochem. Pharmacol.*, 66: 1245–1251 (2003).
- 5) Ding, X. and Kaminsky, L. S.: Human extrahepatic cytochromes P450: function in xenobiotic metabolism and tissue-selective chemical toxicity in the respiratory and gastrointestinal tracts. *Annu. Rev. Pharmacol. Toxicol.*, 43: 149–173 (2003).
- 6) Fernandez-Salguero, P., Hoffman, S. M., Cholerton, S., Mohrenweiser, H., Raunio, H., Rautio, A., Pelkonen, O., Huang, J. D., Evans, W. E., Idle, J. R. and Gonzalez, F. J.: A genetic polymorphism in coumarin 7-hydroxylation: sequence of the human CYP2A genes and identification of variant CYP2A6 alleles. *Am. J. Hum. Genet.*, 57: 651–660 (1995).
- 7) Fujieda, M., Yamazaki, H., Kiyotani, K., Muroi, A., Kunitoh, H., Dosaka-Alkita, H., Sawamura, Y. and Kamataki, T.: Eighteen novel polymorphisms of the CYP2A13 gene in Japanese. *Drug Metab. Pharmacokin.*, 18: 86–90 (2003).

- 8) Zhang, X., Chen, Y., Liu, Y., Ren, X., Zhang, Q. Y., Caggana, M. and Ding, X.: Single nucleotide polymorphisms of the human CYP2A13 gene: evidence for a null allele. *Drug Metab. Dispos.*, 31: 1081–1085 (2003).
- 9) Cauffiez, C., Lo-Guidice, J. M., Quaranta, S., Allorge, D., Chevalier, D., Cenee, S., Hamdan, R., Lhermitte, M., Lafitte, J. J., Libersa, C., Colombel, J. F., Stucker, I. and Broly, F.: Genetic polymorphism of the human cytochrome CYP2A13 in a French population: implication in lung cancer susceptibility. *Biochem. Biophys. Res. Commun.*, 317: 662–669 (2004).
- 10) Smith, B. D., Sanders, J. L., Porubsky, P. R., Lushington, G. H., Stout, C. D. and Scott, E. E.: Structure of the human lung cytochrome P450 2A13. *J. Biol. Chem.*, 282: 17306–17313 (2007).
- 11) Lewis, D. F.: The CYP2 family: models, mutants and interactions. *Xenobiotica*, 28: 617–661 (1998).

Implications of Prenatal Diagnosis of the Fetus With Both Interstitial Deletion and a Small Marker Ring Originating From Chromosome 5

Hiroyasu Ohashi,¹ Kaoru Suzumori,^{1,2*} Yasushi Chisaka,³ Shinichi Sonta,¹ Tomoko Kobayashi,⁴ Yoko Aoki,⁴ Yoichi Matsubara,⁴ Michiko Sone,⁵ and Lisa G. Shaffer⁶

¹Fetal Life Science Center, Ltd., Nagoya, Japan

²Department of Obstetrics and Gynecology, Nagoya City University, Nagoya, Japan

³Department of Obstetrics and Gynecology, Tohoku University, Sendai, Japan

⁴Department of Medical Genetics, Tohoku University, Sendai, Japan

⁵Kagawa National Children's Hospital, Zentsuji, Kagawa, Japan

⁶Signature Genomic Laboratories, Spokane, Washington

Received 5 May 2010; Accepted 2 August 2010

We describe a patient with 47,XY,del(5)(p11p13), +mar observed in prenatal screening. We performed analyses including G-banding, multi-color fluorescent in situ hybridization (mFISH) for fetal chromosome detection. After birth array-based comparative genomic hybridization (aCGH), bacterial artificial chromosome (BAC)-FISH was carried out to define the chromosomal changes precisely. The mFISH revealed that a ring chromosome that had originated from chromosome 5. The aCGH showed that this fetus had a terminal duplication, an interstitial deletion, and a pericentromeric duplication of the short arm of chromosome 5. This complex alteration resulted in partial trisomy 5p15.33–p15.31, partial monosomy 5p14.3–p13.2, and partial trisomy 5p12–p11. To clarify these alterations, we performed BAC-FISH using BAC clones related to deleted and duplicated regions, and found that a derivative (der) chromosome 5 showed the presence of hybridization signals from the duplicated region at 5p15.33 and the loss of hybridization signals from the deleted region at 5p14.2. In addition, FISH analysis confirmed the origin of the marker chromosome. Hybridization signals from the second intervening sequence at 5p13.1, between the deleted region and the pericentric duplicated region, were present on the marker ring chromosome. © 2010 Wiley-Liss, Inc.

Key words: BAC-FISH; microarray analysis; prenatal diagnosis; ring chromosome

INTRODUCTION

When genetic abnormalities are observed during prenatal screening, deletions, and supernumerary ring chromosomes are often seen separately [Gardner and Sutherland, 1996; Ryan et al., 1997; Slavotinek and Kingston, 1997]. Most cases with deletion of autosomes, even that of a tiny segment, are accompanied by clinical symptoms, including mental and developmental retardation; on

How to Cite this Article:

Ohashi H, Suzumori K, Chisaka Y, Sonta S, Kobayashi T, Aoki Y, Matsubara Y, Sone M, Shaffer LG. 2011. Implications of prenatal diagnosis of the fetus with both interstitial deletion and a small marker ring originating from chromosome 5.

Am J Med Genet Part A 155:192–196.

the other hand, there have been examples of cases with deletion of autosomes without any abnormal features [Gardner and Sutherland, 1996; Daniel and Malafiej, 2003; Liehr et al., 2004].

Here, we describe a rare case with both interstitial deletion and a small ring originating from the same chromosome 5 detected prenatally and characterized by molecular cytogenetics. We emphasize the usefulness of molecular cytogenetics involving array-based comparative genomic hybridization (aCGH) and bacterial artificial chromosome (BAC)-fluorescent in situ hybridization BAC-FISH in providing precise information in cases of complex structural abnormality.

CLINICAL REPORT

Amniocentesis requested for advanced maternal age was performed in gestational week 16 on a 42-year-old woman with two

*Correspondence to:

Kaoru Suzumori, M.D., Ph.D., Fetal Life Science Center, 2-22-8 Chikusa, Chikusa-Ku, Nagoya 464-0858, Japan. E-mail: k.suzumori@flsc.jp

Published online 22 December 2010 in Wiley Online Library (wileyonlinelibrary.com).

DOI 10.1002/ajmg.a.33764

normal children. Fetal chromosomes were analyzed by GTG banding and multi-color fluorescent in situ hybridization (mFISH) using cultured amniocytes. After cytogenetic analyses, she was informed that one chromosome 5 with interstitial deletion and a small marker ring chromosome were detected in all the cells. Then, chromosomal analysis of the parents was performed on peripheral blood and showed normal karyotypes. It was difficult to offer additional molecular analyses within a limited term for pregnancy interruption. Ultrasonographic examination at 19 weeks of gestation did not detect any specific abnormality in the fetus. Despite possible unfavorable prognosis informed in genetic counseling, she and her spouse decided against termination of the pregnancy.

The pregnancy was uneventful and she delivered a phenotypically normal boy at 39 weeks of gestation. Apgar score was 8/8 and there were no particular clinical features. Body length, weight, and head circumference were within the normal range: 48 cm, 2,916 g, and 33 cm, respectively. After birth, we received informed consent to examine aCGH and BAC-FISH for further confirmation of the diagnosis.

Developmental, physical, and neurological examinations were normal and he appropriately reached his milestones. At 1 year and 6 months, his developmental quotient (DQ) was 110 (Fig. 1); echocardiography and brain imaging were also normal.

MOLECULAR CYTOGENETIC STUDIES

Chromosome and FISH Analyses

Cultured amniocytes were analyzed using G-banding with 540 bands per haploid number. G-banded chromosomes demonstrated

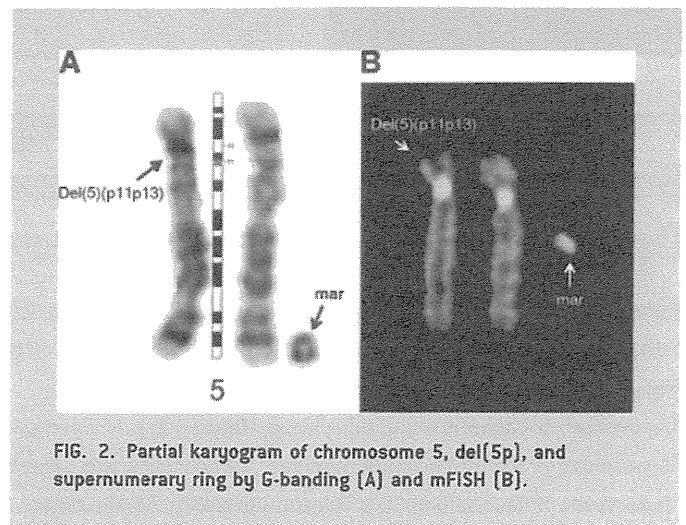


FIG. 2. Partial karyogram of chromosome 5, del(5p), and supernumerary ring by G-banding (A) and mFISH (B).

that all cells had an interstitial deletion of chromosome 5 (5p11 → p13), and a small marker ring chromosome (Fig. 2A). The origin of this marker chromosome was unclear by G-banding. Therefore, the initial karyotyping was 47,XY,del(5)(p11p13),+mar. The mFISH revealed that the marker ring originated from chromosome 5, the same as the deleted chromosome (Fig. 2B). The ring chromosome seemed to have a centromere because this marker was detected in all cells. Chromosome analysis of the parents showed no abnormalities, indicating that these structural abnormalities in the fetus were de novo.

Oligonucleotide aCGH

For detection of gain and loss of chromosome segments, oligonucleotide-based microarray analysis was performed on reserved cultured amniocytes using a 105K-feature whole-genome microarray (Signature Chip Oligo Solution[®], made for Signature Genomic Laboratories by Aligent Technologies Inc., Santa Clara, CA) [Ballif et al., 2008]. Microarray analysis of 1543 loci using on oligonucleotide array detected a complex abnormality in the DNA obtained from cultured amniocytes. Based on microarray analysis, this fetus had two duplications and a deletion of the short arm of chromosome 5. This abnormality was first characterized by a single copy gain of 380 oligonucleotide probes from the terminal end of the short arm of 5p, at 5p15.33p15.31. The extent of this duplication has been estimated to be approximately 6.1 Mb. The second alteration was characterized by a single copy loss of 347 oligonucleotide probes from 5p14.3p13.2. The extent of this interstitial deletion is estimated to be approximately 15.3 Mb. The third alteration was characterized by a single copy gain of 147 oligonucleotide probes from the pericentric region at 5p12p11. The extent of this duplication has been estimated to be approximately 3.4 Mb. Thus, this complex alteration resulted in partial trisomy 5p15.33–p15.31, partial monosomy 5p14.3–p13.2, and partial trisomy 5p12–p11. In conclusion, the result of microarray was arr5p15.33–p15.31(131,945–6,267,160)x3, 5p14.3–p13.2(21,438,495–36,736,934)x1, 5p12–p11(42,529,343–45,908,725)x3 (Fig. 3).

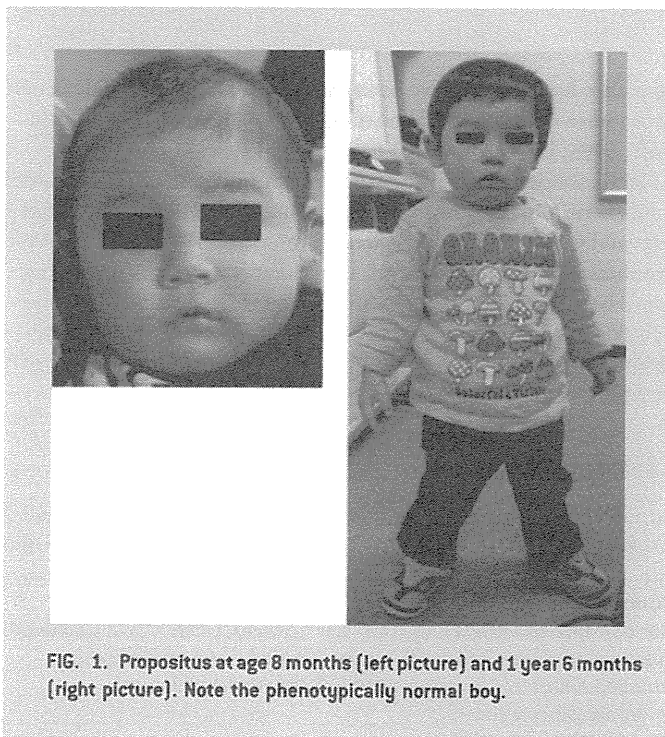


FIG. 1. Propositus at age 8 months (left picture) and 1 year 6 months (right picture). Note the phenotypically normal boy.

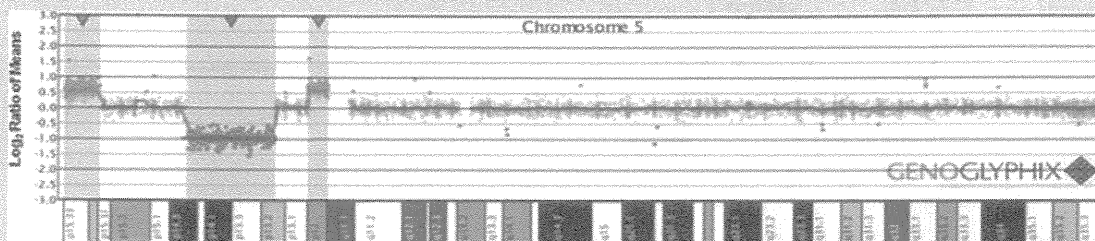


FIG. 3. Microarray plot showing, from left to right, a single copy gain of 380 oligonucleotide probes at 5p15.33p15.31, approximately 6.1 Mb in size; a single copy loss of 347 oligonucleotide probes from 5p14.3p13.2, approximately 15.3 Mb; and single copy gain of 147 oligonucleotide probes at 5p12p11, approximately 3.4 Mb in size. Probes are ordered on the x-axis according to physical mapping positions, with the distal p-arm on the left and the distal q-arm on the right.

BAC-FISH

For confirmation of the array results, FISH analyses were performed with BAC clones from duplicated and deleted regions as previously described [Shaffer et al., 1994; Traylor et al., 2009]. For this study, we used cord blood obtained at delivery.

FISH using a BAC clone from the 5p14.2 deleted region (RP11-701M20) and the 5p15.33 duplicated region (RP11-1006P13) identified an abnormal deleted (del) chromosome 5 that showed the loss of hybridization signals from the deleted region at 5p14.2 (Fig. 4A) and the presence of hybridization signals from the duplicated region at 5p15.33 (Fig. 4C). Interphase FISH

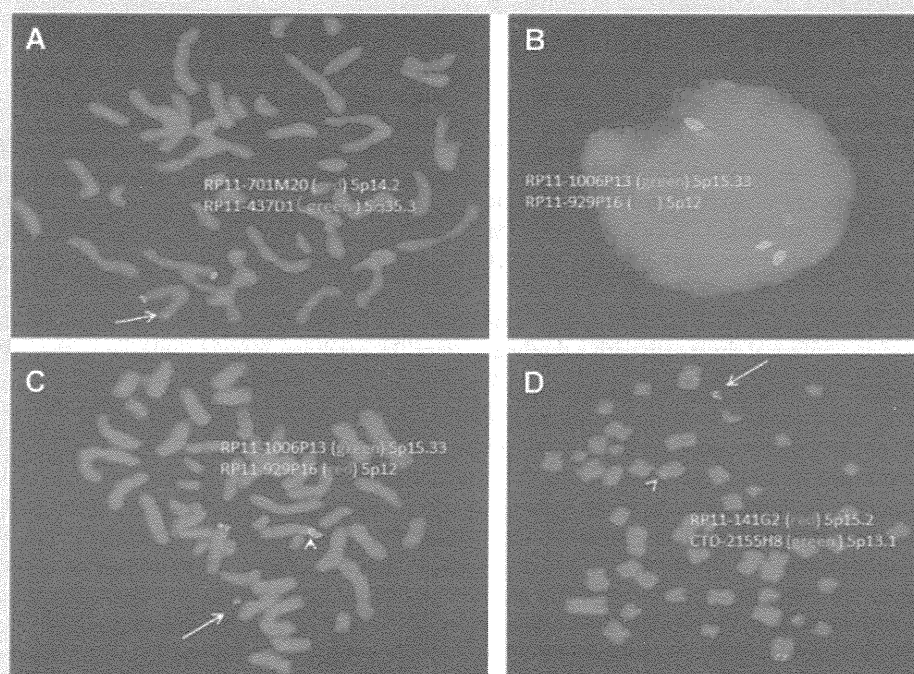


FIG. 4. FISH characterizations of a complex rearrangement on the short arm of chromosome 5. A: FISH showing a deletion of 5p14.2, BAC clone RP11-701M20 from 5p14.2 is labeled in red, and RP11-437D1 from 5q35.3 is labeled in green as a control. The presence of one red signal indicates deletion of 5p14.2 on one homologue (arrow). B,C: FISH with probes from the two regions is shown to be present in three copies by aCGH. BAC clone RP11-1006P13 from 5p15.33 is labeled in green, and RP11-929P16 from 5p12 is labeled in red. Interphase FISH (B) confirmed the presence of three copies of both regions. Metaphase FISH (C) shows a red signal but not a green signal on a small, supernumerary ring chromosome (arrow), indicating the presence of the 5p12 material on the supernumerary chromosome. Dotted green signals from 5p15.33 were present on the normal chromosome 5 homologs, but terminal duplicated signals were observed on one chromosome 5 (arrowhead). D: FISH with probes from the intervening regions shown to be present in two copies by aCGH. BAC clone RP11-141G2 from 5p15.2 is labeled in red, and CTD-2155H8 from 5p13.1 is labeled in green. The supernumerary ring chromosome (arrow) shows a green signal and therefore the presence of material from 5p13.1, while one chromosome 5 homolog (arrowhead) shows a deletion for this region. The probe from 5p15.2 shows a normal hybridization pattern.

we performed FISH analysis using BAC clones from the duplicated 5p15.33, 5p12 regions and deleted 5p14.2 region. The short arm of the del(5) revealed a duplication of 5p15.31 → 5p15.33 and a deletion of 5p13.1 → p14.3. The r(5) was comprised of material from 5p10 → p13.2. Although supernumerary ring chromosome formation is difficult to determine, we speculate that this case have resulted from “centromere misdivision” along with a break in either the p or q arm, forming a small ring chromosome [Baldwin et al., 2008].

In summary, this complex 5p abnormality was characterized by a terminal duplication of 5p15.33p15.31 of approximately 6.4 Mb, an interstitial deletion 15p14.3p13.2 of approximately 15.3 Mb and an interstitial duplication of 5p12p11 of approximately 3.4 Mb. The 5p terminal duplication contained at least 21 genes including ADAMTS16, AHRR, and C5orf38. The 5p14.3p13.2 deletion lacked at least 22 genes including *CDH12*, *PRDM9*, *CDH10*, and *DH9*. The 5p12p11 duplication contained at least 11 genes including *GHR*, *SEPP1*, *C5orf39*, and *ZNF11131*.

When the child was examined at 1 year and 6 months, we could not find any developmental abnormality, either physical or mental. Because of his age he will need to be followed to confirm normal intellectual development. In order to provide accurate and useful genetic counseling in similar cases in the future, the accumulation of further reports with complicated chromosome abnormalities would be beneficial.

REFERENCES

- Baldwin EL, May LE, Justice AN, Martin CL, Ledbetter DH. 2008. Mechanism and consequences of small supernumerary marker chromosomes: From Barbara McClintock to modern genetic-counseling issue. *Am J Hum Genet* 82:398–410.
- Ballif BC, Theisen A, McDonald-McGinn DM, Zackai EH, Bejjani BA, Shaffer LG. 2008. Identification of a previously unrecognized microdeletion syndrome of 16q11.2q12.2. *Clin Genet* 74:469–475.
- Bernardini L, Capalbo A, D’Avanzo MG, Torrente I, Grammatico P, Dell’Edera D, Cavalcanti DP, Novelli A, Dallapiccola B. 2007. Five cases of supernumerary small ring chromosomes 1: Heterogeneity and genotype–phenotype correlation. *Eur J Med Genet* 50:94–102.
- Brøndum-Nielsen K, Mikkelsen M. 1995. A 10-year survey, 1980–1990, of prenatally diagnosed small supernumerary marker chromosomes, identified by FISH analysis. Outcome and follow-up of 14 cases diagnosed in a series of 12,699 prenatal samples. *Prenat Diagn* 15:615–619.
- Callen DF, Eyre H, Lane S, Shen Y, Hansmann I, Spinner N, Zackai E, McDonald-McGinn D, Schuffenhauer S, Wauters J, Van Thienen M-N, Van Roy B, Sutherland GR, Haan EA. 1993. High resolution mapping of interstitial long arm deletions of chromosome 16: Relationship to phenotype. *J Med Genet* 30:828–832.
- Daniel A, Malafiej P. 2003. A series of supernumerary small ring marker autosomes identified by FISH with chromosome probe arrays and literature review excluding chromosome 15. *Am J Med Genet Part A* 117A:212–222.
- Gardner RJM, Sutherland GR. 1996. *Chromosome Abnormalities and Genetic Counseling*. 2nd edition. New York, Oxford: Oxford University Press. pp. 1–478.
- Gereltzul E, Baba Y, Suda N, Shiga M, Inoue MS, Tsuji M, Shin I, Hirata Y, Ohyama K, Moriyama K. 2008. Case report of de novo dup(18p)/del(18q) and r(18) mosaicism. *J Hum Genet* 53:941–946.
- Gutiérrez-Angulo M, Lazalde B, Vasquez AI, Leal C, Corral E, Rivera H. 2002. del(X)(p22.1)/r(X)(p22.1q28) Dynamic mosaicism in a Turner syndrome patient. *Ann Genet* 45:17–20.
- Kara N, Okten G, Gune SO, Saglam Y, Tasdemir HA, Pinarli FA. 2008. An epileptic case with mosaic ring chromosome 6 and 6q terminal deletion. *Epilepsy Res* 80:219–223.
- Karaman B, Aytan M, Yilmaz K, Toksoy G, Onal EP, Ghanbari A, Engur A, Kayserili H, Yuksel-Apak M, Basaran S. 2006. The identification of small supernumerary marker chromosomes; the experiences of 15,792 fetal karyotyping from Turkey. *Eur J Med Genet* 49:207–214.
- Knight LA, Yong MH, Tan M, Ng IS. 1995. Del(3) (p25.3) without phenotypic effect. *J Med Genet* 32:994–995.
- Liehr T, Claussen U, Starke H. 2004. Small supernumerary marker chromosomes (sSMC) in humans. *Cytogenet Genome Res* 107:55–67.
- Mainardi PC, Perfumo C, Cali A, Coucourde G, Pastore G, Cavani S, Zara F, Overhauser J, Pierluigi M, Bricarelli FD. 2001. Clinical and molecular characterization of 80 patients with 5p deletion: Genotype–phenotype correlation. *J Med Genet* 38:151–158.
- Michalski K, Rauer M, Williamson N, Perszyk A, Hoo JJ. 1993. Identification, counselling, and outcome of two cases of prenatally diagnosed supernumerary small ring chromosomes. *Am J Med Genet* 46:88–94.
- Overhauser J, Huang X, Gersh M, Wilson W, McMahon J, Bengtsson U, Rojas K, Meyer M, Wasmuth JJ. 1994. Molecular and phenotypic mapping of the short arm of chromosome 5: Sublocalization of the critical region for the cri-du-chat syndrome. *Hum Mol Genet* 3:247–252.
- Ryan AK, Goodship JA, Wilson DI, Philip N, Levy A, Seidel H, Schuffenhauer S, Oechsler H, Belohradsky B, Prieur M, Aurias A, Raymond FL, Clayton-Smith J, Hatchwell E, McKeown C, Beemer FA, Dallapiccola B, Novelli G, Hurst JA, Ignatius J, Green AJ, Winter RM, Brueton L, Brøndum-Nielsen K, Stewart F, Van Essen T, Patton M, Paterson J, Scambler PJ. 1997. Spectrum of clinical features associated with interstitial chromosome 22q11 deletions: A European collaborative study. *J Med Genet* 34:798–804.
- Schuffenhauer S, Kobelt A, Daumer-Haas C, Löffler C, Müller G, Murken J, Meitinger T. 1996. Interstitial deletion 5p accompanied by dicentric ring formation of the deleted segment resulting in trisomy 5p13-cen. *Am J Med Genet* 65:56–59.
- Shaffer LG, McCaskill C, Han J-Y, Choo KHA, Cuttillo DM, Donnemfeld AE, Weiss L, Van Dyke DL. 1994. Molecular characterization of de novo secondary trisomy 13. *Am J Hum Genet* 55:968–974.
- Slavotinek A, Kingston H. 1997. Interstitial deletion of bands 4q12 → q13.1: Case report and review of proximal 4q deletions. *J Med Genet* 34:862–865.
- Traylor R, Fan Z, Ballif BC. 2009. Microdeletion of 6q16.1 encompassing *EPHA7* in a child with mild neurological abnormalities and dysmorphic features: Case report. *Mol Cytogenet* 2:1–6.
- Weiss A, Shalev S, Weiner E, Shneor Y, Shalev E. 2003. Prenatal diagnosis of 5p deletion syndrome following abnormally low maternal serum human chorionic gonadotrophin. *Prenat Diagn* 23:572–574.

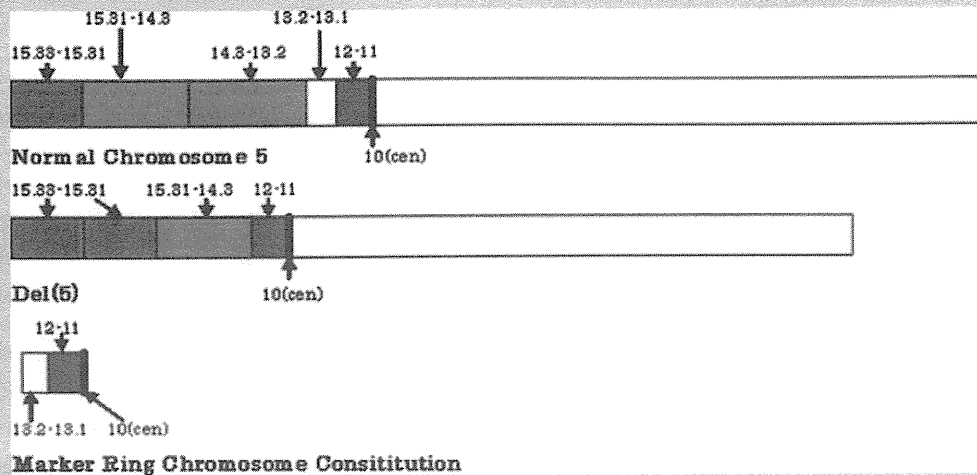


FIG. 5. Molecular background information on the deleted chromosome 5 and marker ring chromosome.

(Fig. 4B) clarified the presence of three copies of 5p15.33 and 5p12 regions. This del(5) also showed hybridization signals in an experiment using BAC clones from the first normal intervening sequence, between the terminal duplication and the deleted region, at 5p15.2 (RP11-141G2; Fig. 4D). Additional FISH analysis using a BAC clone from the 5p12 duplicated region (RP11-929P16) confirmed the origin of the marker ring chromosome (Fig. 4C). Hybridization signals from the second intervening normal sequence at 5p13.1 (CTD-2155H8), between the deleted region and the pericentric duplicated region, were also present on the marker ring chromosome, but not on the del(5), indicating that the deletion on that chromosome extends from 5p14.3 through 5p13.1 (Fig. 4D).

In conclusion, this baby had two abnormal derivative chromosomes. The first der(5) had an abnormal short arm with a duplication of 5p15.31 → 5p15.33, and a deletion of 5p13.1 → p14.3. The second der(5), the marker ring chromosome, was comprised of material from 5p10 → p13.2 (Fig. 5). The final karyotype of the baby is: 47,XY,ish der(5)(pter → p15.31::pter → p14.3::p11 → qter)(RP11-1006P13++,RP11-141G2+,RP11-701M20-,CTD-2155H8-),+der(5):(13.2 → p10):(CTD-2155H8+,RP11-929P16+).

DISCUSSION

Partial deletion of 5p is often seen in prenatal diagnoses and newborn analyses [Mainardi et al., 2001; Weiss et al., 2003]. In autosomes other than chromosome 5, deletions involving various chromosomes have also been reported in the literature [Gardner and Sutherland, 1996; Ryan et al., 1997; Slavotinek and Kingston, 1997]. Partial deletion of autosomes is generally accompanied by mild-to-severe clinical symptoms, including mental and developmental retardation in babies, although there have been exceptional cases where no clinical symptoms are observed [Callen et al., 1993; Overhauser et al., 1994; Knight et al., 1995]. Supernumerary marker chromosomes including small rings are also seen frequently in prenatal diagnoses [Michalski et al., 1993; Brøndum-Nielsen and

Mikkelsen, 1995; Karaman et al., 2006]. Among babies with such small markers, some cases have no clinical features, but others showed mild-to-severe abnormalities after birth [Callen et al., 1993; Overhauser et al., 1994; Knight et al., 1995; Gardner and Sutherland, 1996; Daniel and Malafiej, 2003; Liehr et al., 2004; Bernardini et al., 2007]. Thus, in genetic counseling, it is important to offer chromosomal information from prenatal diagnoses and to provide as much detail as possible, including the origin and inheritance.

The present case had a deletion and a supernumerary marker ring chromosome. To our knowledge, this is the first report of detection by prenatal screening of both a deletion and a marker ring. In the literature, there are some mosaic cases of clones with a deletion and an additional ring separately [Gutiérrez-Angulo et al., 2002; Gereltzul et al., 2008; Kara et al., 2008], but such cases are extremely rare. In newborn infants, only one other case has been reported [Schuffenhauer et al., 1996] with a deletion and a ring of chromosome 5; this baby showed a mosaicism of 46,XY,del(5)/47,XY,del(5),+dic(5), with macrocephaly, asymmetric square skull, minor facial anomalies, omphalocele, inguinal hernias, hypospadias, and club feet. The break points of the deletion shared cen and p13 with those of the dicentric ring chromosome; this case had partial duplication of 5p (p13 → cen), and the mechanisms of del(5) and dic(5) were relatively straightforward. In the present case, on the other hand, the mechanisms of del(5) and marker ring [r(5)] were extremely complex. Microarray analysis revealed a terminal duplication, an interstitial deletion, and a pericentromeric duplication of the short arm of chromosome 5. Through this analysis, a total of six break points of the short arm of chromosome 5 (p15.33, p15.31, p14.3, p13.2, p12, and p11) were related to the formation of the structural abnormality with the duplication and the deletion, and the marker ring. According to the results of the G-band analysis of this case, we determined the break points of del(5) to be p11 and p13. However, assuming the microarray data are correct, the composition of r(5) becomes complicated, and explanation of the underlying mechanisms becomes difficult. To facilitate understanding of the exact composition of del(5) and r(5),

Original article

A familial case of LEOPARD syndrome associated with a high-functioning autism spectrum disorder

Yoriko Watanabe^{a,1,*}, Shoji Yano^b, Tetsuya Niihori^c, Yoko Aoki^c,
Yoichi Matsubara^c, Makoto Yoshino^u, Toyojiro Matsuishi^{a,1}

^a Department of Pediatrics and Child Health, Kurume University School of Medicine, 67 Asahi-machi, Kurume, Japan

^b Genetics Division, Department of Pediatrics, LAC+USC Medical Center, Keck School of Medicine, University of Southern California, Los Angeles, CA, USA

^c Department of Medical Genetics, Tohoku University School of Medicine, Sendai, Japan

Received 6 July 2010; received in revised form 3 October 2010; accepted 6 October 2010

Abstract

A connection between LEOPARD syndrome (a rare autosomal dominant disorder) and autism spectrum disorders (ASDs) may exist. Of four related individuals (father and three sons) with LEOPARD syndrome, all patients exhibited clinical symptoms consistent with ASDs. Findings included aggressive behavior and impairment of social interaction, communication, and range of interests. The coexistence of LEOPARD syndrome and ASDs in the related individuals may be an incidental familial event or indicative that ASDs is associated with LEOPARD syndrome. There have been no other independent reports of the association of LEOPARD syndrome and ASDs. Molecular and biochemical mechanisms that may suggest a connection between LEOPARD syndrome and ASDs are discussed.

© 2010 The Japanese Society of Child Neurology. Published by Elsevier B.V. All rights reserved.

Keywords: LEOPARD syndrome, Noonan syndrome; Autism spectrum disorders (ASDs); RAS/MAPK signal transduction pathway

1. Introduction

LEOPARD syndrome (OMIM#151100) is a rare autosomal dominant disorder characterized by Lentiginos, Electrocardiogram abnormalities, Ocular hypertelorism, Pulmonic valvular stenosis, Abnormalities of genitalia, Retardation of growth, and Deafness. This syndrome is caused by germline missense mutations in the *PTPN11* gene that encodes Src homology 2 domain-containing tyrosine phosphatase 2 (Shp2): non-receptor protein-tyrosine phosphatase comprising two N-terminal SH2 domains, a catalytic domain, and a C

terminus with tyrosylphosphorylation sites and a proline-rich stretch. The mutations induce catalytically impaired Shp2 by a “dominant negative effect” [1–2].

In the more common Noonan syndrome, approximately 50% of patients have *PTPN11* mutations scattered over the entire Shp2, including the catalytic domain. The mutations resulting in the Noonan phenotype are the “gain-of-function” mutations, and they exhibit substantially increased catalytic ability. Although LEOPARD syndrome and Noonan syndrome are caused by *PTPN11* mutations resulting in opposite effects, they share many common clinical features, including physical dysmorphic findings and intellectual disability [1].

The term “autism spectrum disorders (ASDs)” was first used by Lorna Wing [3] and then widely used as a category comprised of autistic disorder, Asperger’s

* Corresponding author. Tel.: +81 942 35 3311x.3656; fax: +81 942 38 1792.

E-mail address: york@med.kurume-u.ac.jp (Y. Watanabe).

¹ The author contributed equally to this work.

disorder, and other related conditions [4]. These conditions are very common neurobehavioral disorders that are characterized by impairments in three behavioral domains, including social interaction, language/communication/imaginative play, and a range of interests and activities [3–5].

At least ten genes have been reported to be associated with ASDs [6]. Except for Rett syndrome, the other pervasive developmental disorder (PDD) subtypes including autistic disorder, Asperger's disorder, disintegrative disorder, and PDD Not Otherwise Specified (PDDNOS) are not tightly linked to any particular gene mutations. Several common genetic syndromes are known to be associated with ASDs. Autism is frequent in patients with tuberous sclerosis (TSC) [7], with neurofibromatosis type 1 [8,9] and with Fragile X syndrome [10]. Studies of psychological profiles of adults with Noonan syndrome did not suggest a specific behavioral phenotype, but difficulties with social competence and emotional perceptions were noted [11]. A case of Noonan syndrome who was also diagnosed with autism was reported [12]. The present study of neuropsychiatric evaluation in a familial case of LEOPARD syndrome indicates all patients satisfied the criteria of ASDs. An association of LEOPARD syndrome and ASDs has not been reported previously. The familial case presented in this report may suggest such an association.

2. Patients and methods

After obtaining written informed consent, fifteen coding exons in *PTPN11* were sequenced in each patient following the methods described somewhere else [13].

Diagnostic and Statistical Manual of Mental Disorders, Fourth Edition (DSM-IV-TR) [5] and The high-functioning Autism Spectrum Screening Questionnaire (ASSQ) [14] were used in neuropsychiatric evaluation of the subjects.

Patient 1 is a 20-year-old male who was born as the second child to a non-consanguineous Japanese couple. His early developmental milestones were reportedly unremarkable. He was clinically diagnosed with LEOPARD syndrome at age 7 years based on findings that included lentigines, multiple café-au-lait spots, electrocardiogram (ECG) abnormalities, ventricular septal defect, ocular hypertelorism, short stature, and unilateral renal hypoplasia. *PTPN11* mutation analysis revealed a heterozygous mutation of 1403C > T (T468 M). The patient was diagnosed as having Asperger's disorder based on ASSQ and DSM-IV-TR, at age 12 years. His intelligence quotient (IQ) by the Wechsler Intelligence Scale for Children-third edition (WISC-III) was 85 (verbal: 77, performance 98). His ASSQ score by mother's rating was 41. He met the DSM-IV-TR diagnostic criteria of Asperger's disorder with all subcategories in the category of Qualitative impairment in social interaction

(Category 1), three subcategories (1, 2, and 4) in the category of Restricted repetitive and stereotyped patterns of behavior, interests and activities (Category 2), and the rest of the four categories (Table 1).

Patient 2 is a 15-year-old younger brother of Patient 1. His early infantile developmental milestones were unremarkable. He was diagnosed with growth retardation at age 2½ years. At age 12 years his clinical findings of a few café-au-lait spots, ocular hypertelorism, and undescended testes led us to obtain *PTPN11* mutation analysis, which showed the same heterozygous mutation of 1403C > T. At age 9 years, a diagnosis of Asperger's disorder was made based on ASSQ and DSM-IV-TR. His full-scale IQ by WISC-III at age 9 years was 99 (verbal 104, performance 92). His ASSQ score by parental rating was 32 at age 15 years. He also met the Asperger's disorder diagnostic criteria with all subcategories of Category 1, three of Category 2 (1, 2, and 4), and the rest of the categories (Table 1).

Patient 3 is the 22-year-old eldest brother of Patients 1 and 2. His developmental milestones were normal, although his ritualistic behavior and difficulties in relating to peers were noted in his childhood. He had a surgical repair of bilateral undescended testes and inguinal hernia. He was diagnosed with Wolff-Parkinson-White syndrome at age nine years. He has ocular hypertelorism and short stature. The same *PTPN11* heterozygous mutation found in the two younger siblings was identified in this patient. He attends college, and was diagnosed as having PDDNOS, because he also had impaired development of reciprocal social interaction associated with communication skills, repetitive routine, and ritualistic behavior. His ASSQ score was 7 at age 22 years (Table 1).

Patient 4 is a 55-year-old male who is the father of the siblings. He has prominent lentigines, bilateral mild hearing loss, cardiac anomalies, ECG abnormalities, short stature, and apparent ocular hypertelorism. His early developmental milestones are not well known. He has been noted to have obsession with a specific topic, repetitive routine and rituals, and clumsy movements. At age 50 years, his social skills and aggressive behavior were noted to be deteriorating, and consequently he was suspected of having Asperger's disorder based on DSM-IV-TR. He met the diagnostic criteria of Asperger's disorder with Category 1 (1 and 3), Category 2 (1 and 2), and the rest of the four categories. His ASSQ score was 20 at age 55 years by his wife's evaluation. He has the same heterozygous *PTPN11* mutation (Table 1).

3. Discussion

The presented familial case of LEOPARD syndrome included individuals (patients 1, 2, and 4) diagnosed with or suspected of having Asperger's disorder, and

Table 1
Summary of clinical findings and *PTPN11* mutation.

	Pt. 1 Male	Pt. 2 Male	Pt. 3 Male	Pt. 4 Male
Age	20 y	15 y	22 y	55 y
<i>Physical findings</i>				
Skin: café-au-lait spots	multiple	a few	a few	a few
Lentiginosities	+++	+++	-	+++
Cardiac defects	VSD	No	No	No
EKG abnormalities	+	No	WPW	No
Ocular hypertelorism	+	+	+	+
Pulmonary stenosis	No	No	No	No
Abnormal genitalia	No	Und. Testes ^o	Und. Testes ^o	No
Renal anomalies	R-hypoplasia	No	No	No
Retardation of growth	Yes	+	+	No
Deafness	No	No	No	Yes
<i>Miscellaneous:</i>				
Rocker bottom feet	Yes	Yes	Yes	No
Macrocephaly	Yes	Yes	Yes	No
<i>PTPN11</i> mutation	T468 M	T468 M	T468 M	T468 M
<i>Neuropsychological</i>				
Diagnosis	AD ^{**}	AD ^{**}	PDDNOS ^{***}	AD ^{**}
ASSQ score ⁽¹⁾ (age)	41 (12 y)	32 (15 y)	7 (22 y)	20 (50 y)
WISC-III ⁽²⁾ (age)	85 (12 y)	99 (9 y)	n/a	n/a
Verbal/performance	77/98	104/92	n/a	n/a

^o Und. Testes, undescended testes.

^{**} AD, Asperger's disorder.

^{***} PDDNOS, Pervasive developmental disorder not otherwise specified.

⁽¹⁾ ASSQ score, Autism Spectrum Screening Questionnaire Score. The cutoff score of 3 predicts 91% of the true positive rate of Autistic spectrum disorders.

⁽²⁾ WISC-III, Wechsler Intelligence Scale for Children-third edition.

patient 3 was diagnosed as having PDDNOS, which may lead to the diagnosis of ASD. ASDs were first introduced by Lorna Wing, who suggested that Asperger's disorder is a type of ASD and described in detail its various manifestations in speech, nonverbal communication, social interaction, motor coordination, motor clumsiness, and idiosyncratic interests [3]. Patient 3 did not have enough clinical symptoms to meet the diagnostic criteria for Asperger's disorder; however, he had some symptoms suggestive of ASD in his childhood that led to a diagnosis of PDDNOS.

The ASSQ is a 27-item checklist for completion by lay informants when assessing characteristic symptoms of Asperger's disorder and high-functioning autism in children and adolescents with normal intelligence or mild mental retardation. The ASSQ allows for rating on a 3-point scale (0, 1, or 2; 0 indicating normality, 1 some abnormality, and 2 definite abnormality). The range of possible scores is 0–54. The mean ASSQ parent scores in the Asperger's disorder validation sample were 25.1 (SD, 7.3) [14]. The cutoff score of 13 is 91% of the true positive rate of ASDs. The ASSQ score was established as a screening tool primarily for children between 6 and 17 years of age by parents and/or teachers. The delayed evaluation of patient 3 may account for the difference in diagnosis between this patient and his siblings.

ASDs are known to be associated with particular genetic disorders such as fragile X syndrome [10,15,

16], tuberous sclerosis (TSC) [7], and neurofibromatosis type 1 [8,9]. Fifty percent of children with TSC have behavioral problems in the form of ASDs. Gene mutations in either *TSC1* or *TSC2* influence neural precursors, resulting in abnormal cell differentiation and dysregulated control of cell size. These cells migrate to the cortex to generate an abnormal collection of inappropriately positioned neurons, causing widespread cortical disorganization and structural abnormalities [7]. Mutations in *PTPN11* causing LEOPARD syndrome induce catalytically impaired Shp2. In situ hybridization detected Shp2 expression in the neural ectoderm and nervous system in mouse embryos, suggesting an involvement of Shp2 in neural development. Shp2 is a critical signaling molecule in the coordinated regulation of progenitor cell proliferation and neuronal/astroglial cell differentiation. The studies with mutant mouse strains with Shp2 selectively deleted in neural precursor cells showed a dramatic phenotype of growth retardation, early postnatal lethality, and multiple defects in proliferation and cell fate specification in neural stem/progenitor cells [17]. The product of the *TSC2* gene tuberin is known to up-regulate the B-RAF/MEK/MAPK signal transduction pathway. B-RAF is required for neuronal differentiation, suggesting another possible link between B-RAF signaling and the clinical manifestations of TSC including ASDs [18]. Disturbed neuronal cell differentiation and development due to mutations in

the TSC genes and the *PTPN11* gene are likely to contribute to the development of ASDs in patients with these syndromes.

NF-1 is well known to be associated with ASDs. The prevalence of autism in patients with NF-1 was reported to be 4% [9]. The well-known function of the NF-1 protein is to act as a RAS-GTPase-activating protein known to be involved in the regulation of the RAS-mitogen-activated protein kinase (MAPK) pathway. Mutations in the NF-1 gene are thought to result in activation of the RAS/MAPK signal transduction pathway [2]. Clinical overlap between LEOPARD syndrome and NF-1 is also well known [19].

Approximately 50% of patients with Noonan syndrome are due to missense *PTPN11* mutations [20]. *PTPN11* encodes SHP2, a protein tyrosine phosphatase, that is involved in the activation of the RAS/MAPK cascade [2]. Noonan syndrome is caused by “gain of function” *PTPN11* mutations [1,2], and the SHP2 mutants due to the *PTPN11* mutations causing Noonan syndrome cause prolonged activation of the RAS/MAPK pathway [2]. Schubbert et al. [21] reported that germline KRAS mutations cause Noonan syndrome through the hyperactive RAS/MAPK pathway.

Herault et al. [22] reported a positive association of the HRAS gene and autism. The psychological profiles of adults and children with Noonan syndrome have been studied, and deficiencies in social and emotional recognition and expression have been identified in adults, while low verbal IQ, clumsiness, and impairment of developmental coordination have been reported in children [23].

To date, there have been no reports to suggest an association of LEOPARD syndrome and ASDs. Our observations in this familial case may suggest at least some degree of association between LEOPARD syndrome and ASD phenotypes possibly through the RAS/MAPK signal transduction pathway. Further studies with more patients with LEOPARD syndrome are needed to establish the association and to investigate the genetic contributing factors causing ASDs, leading to the prevention and earlier detection of ASDs and better management of patients with these disorders.

References

- [1] Kontaridis M, Swanson KD, David FS, Barford D, Neel BG. PTPN11 (Shp2) mutations in LEOPARD syndrome have dominant negative, not activating, effects. *J Biol Chem* 2006;281: 6785–92.
- [2] Aoki Y, Niihori T, Narumi Y, Kure S, Matsubara Y. The RAS/MAPK syndromes: novel roles of the RAS pathway in human genetic disorders. *Hum Mutat* 2008;29:992–1006.
- [3] Wing L. Autistic spectrum disorders. *BMJ* 1996;312:327–8.
- [4] Khouzam HR, El-Gabalawi F, Pirwani N, Priest F. Asperger's disorder: a review of its diagnosis and treatment. *Comp Psychiatr* 2004;45:181–91.
- [5] American Psychiatric Association. Diagnostic and Statistical Manual of Mental Disorders. 4th ed.-Text Revision. Washington, DC: American Psychiatric Association; 2000.
- [6] Muhle R, Trentacose SV, Rapin I. The genetics of autism. *Pediatrics* 2004;113:e472–86.
- [7] Curatolo P. Tuberous sclerosis: genes, brain, and behavior. *Dev Med Child Neurol* 2006;48:404.
- [8] Gillberg C, Forsell C. Childhood psychosis and neurofibromatosis—More than a coincidence? *J Autism Dev Disord* 1984;14: 1–8.
- [9] Williams PG, Hersh JH. The association of neurofibromatosis Type 1 and autism. *J Autism Dev Disord* 1998;28:567–71.
- [10] Cohen IL, Sudhalter V, Pfadt A, Jenkins EC, Brown WT, Vietze PM. Why are autism and the fragile-X syndrome associated? Conceptual and methodological issues. *Am J Hum Genet* 1991;48:195–202.
- [11] Verhoeven W, Wingbermuehle E, Egger J, Van der Burgt I, Tuinier S. Noonan syndrome: psychological and psychiatric aspects. *Am J Med Genet A* 2008;146A:191–6.
- [12] Ghaziuddin M, Bolyard B, Alessi N. Autistic disorder in Noonan syndrome. *J Intell Disabil Res* 1994;38:67–72.
- [13] Niihori T, Aoki Y, Ohashi H, Kurosawa K, Kondoh T, Ishikiriyama S, et al. Functional analysis of PTPN11/SHP-2 mutants identified in Noonan syndrome and childhood leukemia. *J Hum Genet* 2005;50:192–202.
- [14] Ehlers S, Gillberg C, Wing L. A screening questionnaire for Asperger syndrome and other high-functioning autism spectrum disorders in school age children. *J Autism Dev Disord* 1999;29:129–41.
- [15] Wahlstrom J, Gillberg C, Gustavson KH, Holmgren G. A Swedish multicenter study. *Am J Med Genet* 1986;23:403–8.
- [16] Tranebjaerg L, Kure P. Prevalence of fra (X) and other specific diagnoses in autistic individuals in a Danish county. *Am J Med Genet* 1991;38:212–4.
- [17] Ke Y, Zhang EE, Hagihara K, Wu D, Pang Y, Klein R, et al. Deletion of Shp2 in the brain leads to defective proliferation and differentiation in neural stem cells, and early postnatal lethality. *Mol Cell Biol* 2007;27:6706–17.
- [18] Karbowiczek M, Cash T, Cheung M, Robertson GP, Astrinidis A, Henske EP. Regulation of B-Raf kinase activity by Tuberin and Rheb is mammalian target of Rapamycin (mTOR)-independent. *J Biol Chem* 2004;279:29930–7.
- [19] Sarkozy A, Conti E, Digilio MC, Marino B, Morini E, Pacileo G, et al. *J Med Genet* 2004;41:e68.
- [20] Tartaglia M, Mehler EL, Goldberg R, Zampino G, Brunner HG, Kremer H, et al. Mutations in PTPN11, encoding the protein tyrosine phosphatase SHP-2, cause Noonan syndrome. *Nat Genet* 2001;29:465–8.
- [21] Schubbert S, Zenker M, Rowe SL, Boll S, Klein C, Bollag G, et al. Germline KRAS mutations cause Noonan syndrome. *Nat Genet* 2006;38:331–6.
- [22] Herault J, Petit E, Martineau J, Perrot A, Lenoir P, Cherpi C, et al. Autism and genetics: clinical approach and association study with two markers of HRAS gene. *Am J Med Genet* 1995;60:276–81.
- [23] Lee DA, Portnoy S, Hill P, Gillberg C, Patton MA. Psychological profile of children with Noonan syndrome. *Dev Med Child Neurol* 2005;47:35–8.

ORIGINAL ARTICLE

A genome-wide association study identifies *RNF213* as the first Moyamoya disease gene

Fumiaki Kamada¹, Yoko Aoki¹, Ayumi Narisawa^{1,2}, Yu Abe¹, Shoko Komatsuzaki¹, Atsuo Kikuchi³, Junko Kanno¹, Tetsuya Niihori¹, Masao Ono⁴, Naoto Ishii⁵, Yuji Owada⁶, Miki Fujimura², Yoichi Mashimo⁷, Yoichi Suzuki⁷, Akira Hata⁷, Shigeru Tsuchiya³, Teiji Tominaga², Yoichi Matsubara¹ and Shigeo Kure^{1,3}

Moyamoya disease (MMD) shows progressive cerebral angiopathy characterized by bilateral internal carotid artery stenosis and abnormal collateral vessels. Although ~15% of MMD cases are familial, the MMD gene(s) remain unknown. A genome-wide association study of 785 720 single-nucleotide polymorphisms (SNPs) was performed, comparing 72 Japanese MMD patients with 45 Japanese controls and resulting in a strong association of chromosome 17q25-ter with MMD risk. This result was further confirmed by a locus-specific association study using 335 SNPs in the 17q25-ter region. A single haplotype consisting of seven SNPs at the *RNF213* locus was tightly associated with MMD ($P=5.3 \times 10^{-10}$). *RNF213* encodes a really interesting new gene finger protein with an AAA ATPase domain and is abundantly expressed in spleen and leukocytes. An RNA *in situ* hybridization analysis of mouse tissues indicated that mature lymphocytes express higher levels of *Rnf213* mRNA than their immature counterparts. Mutational analysis of *RNF213* revealed a founder mutation, p.R4859K, in 95% of MMD families, 73% of non-familial MMD cases and 1.4% of controls; this mutation greatly increases the risk of MMD ($P=1.2 \times 10^{-43}$, odds ratio=190.8, 95% confidence interval=71.7–507.9). Three additional missense mutations were identified in the p.R4859K-negative patients. These results indicate that *RNF213* is the first identified susceptibility gene for MMD.

Journal of Human Genetics (2011) 56, 34–40; doi:10.1038/jhg.2010.132; published online 4 November 2010

INTRODUCTION

'Moyamoya' is a Japanese expression for something hazy, such as a puff of cigarette smoke drifting in the air. In individuals with Moyamoya disease (MMD), there is a progressive stenosis of the internal carotid arteries; a fine network of collateral vessels, which resembles a puff of smoke on a cerebral angiogram, develops at the base of the brain (Figure 1a).^{1,2} This steno-occlusive change can cause transient ischemic attacks and/or cerebral infarction, and rupture of the collateral vessels can cause intracranial hemorrhage. Children under 10 years of age account for nearly 50% of all MMD cases.³

The etiology of MMD remains unclear, although epidemiological studies suggest that bacterial or viral infection may be implicated in the development of the disease.⁴ Growing attention has been paid to the upregulation of arteriogenesis and angiogenesis associated with MMD because chronic ischemia in other disease conditions is not always associated with a massive development of collateral vessels.^{5,6} Several angiogenic growth factors are thought to have functions in the development of MMD.⁷

Several lines of evidence support the importance of genetic factors in susceptibility to MMD.⁸ First, 10–15% of individuals with MMD

have a family history of the disease.⁹ Second, the concordance rate of MMD in monozygotic twins is as high as 80%.¹⁰ Third, the prevalence of MMD is 10 times higher in East Asia, especially in Japan (6 per 100 000 population), than in Western countries.³ Familial MMD may be inherited in an autosomal dominant fashion with low penetrance or in a polygenic manner.¹¹ Linkage studies of MMD families have revealed five candidate loci for an MMD gene: chromosomes 3p24–26,¹² 6q25,¹³ 8q13–24,¹⁰ 12p12–13¹⁰ and 17q25.¹⁴ However, no susceptibility gene for MMD has been identified to date.

We collected 20 familial cases of MMD to investigate linkage in the five putative MMD loci. However, a definitive result was not obtained for any of the loci. We then hypothesized that there might be a founder mutation among Japanese patients with MMD because the prevalence of MMD is unusually high in Japan.¹⁵ Genome-wide and locus-specific association studies were performed and successfully identified a single gene, *RNF213*, linked to MMD. We report here a strong association between MMD onset and a founder mutation in *RNF213*, as well as the expression profiles of *RNF213*, in various tissues.

¹Department of Medical Genetics, Tohoku University School of Medicine, Sendai, Japan; ²Department of Neurosurgery, Tohoku University School of Medicine, Sendai, Japan; ³Department of Pediatrics, Tohoku University School of Medicine, Sendai, Japan; ⁴Department of Pathology, Tohoku University School of Medicine, Sendai, Japan; ⁵Department of Microbiology and Immunology, Tohoku University School of Medicine, Sendai, Japan; ⁶Department of Organ Anatomy, Yamaguchi University Graduate School of Medicine, Ube, Japan and ⁷Department of Public Health, Graduate School of Medicine, Chiba University, Chiba, Japan

Correspondence: Dr S Kure, Department of Pediatrics, Tohoku University School of Medicine, 1-1 Seiryō-machi, Aoba-ku, Miyagi, Sendai 980-8574, Japan.

E-mail: kure@med.tohoku.ac.jp

Received 30 September 2010; accepted 1 October 2010; published online 4 November 2010

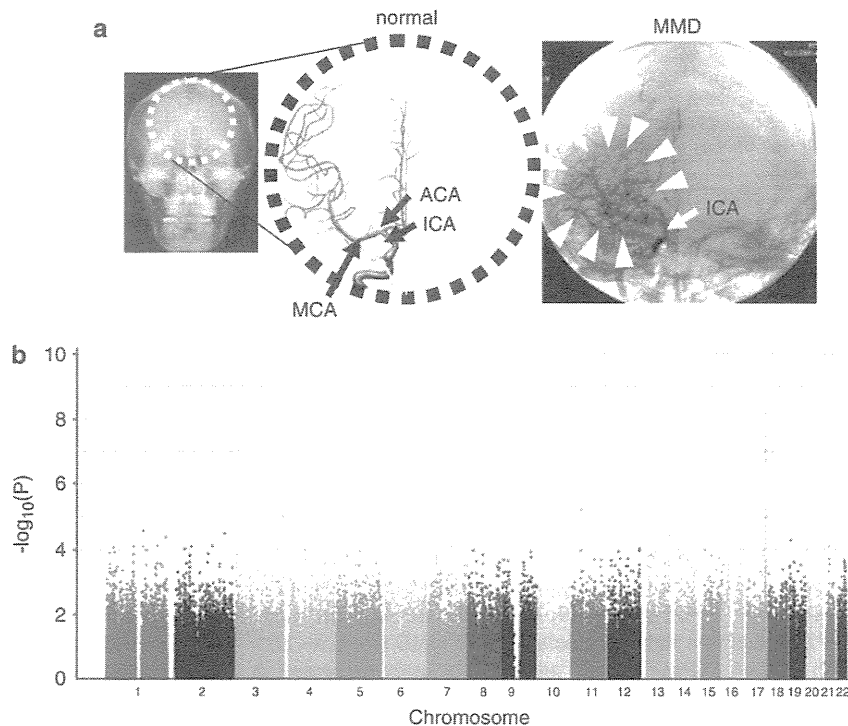


Figure 1 (a) Abnormal brain vessels in MMD. The dotted circle indicates the X-ray field of cerebral angiography (left panel). Normal structures of the right internal carotid artery (ICA), anterior cerebral artery (ACA) and middle cerebral artery (MCA) are illustrated (middle panel). The arrowheads indicate abnormal collateral vessels appearing like a puff of smoke in the angiogram of an individual with MMD (right panel). Note that ACA and MCA are barely visible, because of the occlusion of the terminal portion of the ICA. (b) Manhattan plot of the 785 720 SNPs used in the genome-wide association analysis of MMD patients. Note that the SNPs in the 17q25-ter region reach a significance of $P < 10^{-8}$.

MATERIALS AND METHODS

Affected individuals

Genomic DNA was extracted from blood and/or saliva samples obtained from members of the families with MMD (Supplementary Figure 1), MMD patients with no family history and control subjects. All of the subjects were Japanese. MMD was diagnosed on the basis of guidelines established by the Research Committee on Spontaneous Occlusion of the Circle of Willis of the Ministry of Health and Welfare of Japan. This study was approved by the Ethics Committee of Tohoku University School of Medicine. Total RNA samples were purified from leukocytes using an RNeasy mini kit (Qiagen, Hilden, Germany) and used as templates for cDNA synthesis with an Oligo (dT)₂₀ primer and SuperScript II reverse transcriptase according to the manufacturer's instructions (Invitrogen, Carlsbad, CA, USA).

Linkage analysis

For the linkage analysis, DNA samples were genotyped for 36 microsatellite markers within five previously reported MMD loci using the ABI 373A DNA Sequencer (Applied Biosystems, Foster City, CA, USA). Pedigrees and haplotypes were constructed with the Cyrillic version 2.1 software (Oxfordshire, UK). Multipoint analyses were conducted using the GENEHUNTER 2 software (<http://www.broadinstitute.org/ftp/distribution/software/genehunter/>). Statistical analysis was performed with SPSS version 14.0J (SPSS, Tokyo, Japan).

Genome-wide and locus-specific association studies

A genome-wide association study was performed using a group of 72 MMD patients, which consisted of 64 patients without a family history of MMD and 8 probands of MMD families. The Illumina Human Omni-Quad 1 chip (Illumina, San Diego, CA, USA) was used for genotyping, and single-nucleotide polymorphisms (SNPs) with a genotyping completion rate of 100% were used for further statistical analysis (785 720 out of 1 140 419 SNPs). Genotyping data

from 45 healthy Japanese controls were obtained from the database at the International HapMap Project web site. The 785 720 SNPs were statistically analyzed using the PLINK software (<http://pngu.mgh.harvard.edu/~purcell/plink/index.shtml>). For a locus-specific association study, we used 63 DNA samples consisting of 58 non-familial MMD patients and 5 probands of MMD families. A total of 384 SNPs within chromosome 17q25-ter were genotyped (Supplementary Table 1), using the GoldenGate Assay and a custom SNP chip (Illumina). Genotyping data for 45 healthy Japanese were used as a control. Case-control single-marker analysis, haplotype frequency estimation and significance testing of differences in haplotype frequency were performed using the Haploview version 3.32 program (<http://www.broad.mit.edu/mpg/haploview/>).

Mutation detection

Mutational analyses of *RNF213* and *FLJ35220* were performed by PCR amplification of each coding exon and putative promoter regions, followed by direct sequencing. Genomic sequence data for the two genes were obtained from the National Center for Biotechnology Information web site (<http://www.ncbi.nlm.nih.gov/>) for design of exon-specific PCR primers. *RNF213* cDNA fragments were amplified from leukocyte mRNA for sequencing analysis. Sequencing of the PCR products was performed with the ABI BigDye Terminator Cycle Sequencing Reaction Kit using the ABI 310 Genetic Analyzer. Identified base changes were screened in control subjects. Statistical difference of the carrier frequency of each base change was estimated by Fisher's exact test (the MMD group vs the control group).

Quantitative PCR

MTC Multiple Tissue cDNA Panels (Clontech Laboratory, Madison, WI, USA) were the source of cDNAs from human cell lines, adult and fetal tissues. Mononuclear cells and polymorphonuclear cells were isolated from the fresh peripheral blood of healthy human adults using Polymorphprep (Cosmo Bio,

Carlsbad, CA, USA). T and B cells were isolated from the fresh peripheral blood of healthy human adults using the autoMACS separator (Milteny Biotec, Bergisch Gladbach, Germany). Total RNA was isolated from these cells with the RNeasy Mini Kit (Qiagen) following the manufacturer's instructions. We reverse transcribed 100 ng samples of total RNA into cDNAs using the High Capacity cDNA Reverse Transcription Kit (Applied Biosystems). Quantitative PCRs were performed in a final volume of 20 μ l using the FastStart TaqMan Probe Master (Roche) (Roche, Madison, WI, USA), 5 μ l of cDNA, 10 μ M of RNF- or GAPDH-specific primers and 10 μ M of probes (Universal ProbeLibrary Probe #80 for RNF213 and Roche Probe #60 for GAPDH). All reactions were performed in triplicate using the ABI 7500 Real-Time PCR system (Applied Biosystems). Cycling conditions were 2 min at 50°C and 10 min at 95°C, followed by 40 cycles of 15 s at 95°C and 60 s at 60°C. Real-time PCR data were analyzed by the SDS version 1.2.1 software (Applied Biosystems). We evaluated the relative level of RNF213 mRNA by determining the C_T value, the PCR cycle at which the reporter fluorescence exceeded the signal baseline. GAPDH mRNA was used as an internal reference for normalization of the quantitative expression values.

Multiplex PCR

MTC Multiple Tissue cDNA Panels (Clontech) were the source of human cell lines and cDNAs from human adult and fetal tissues. Multiplex PCRs were performed in a final volume of 20 μ l using the Multiplex PCR Master Mix (Qiagen), 2 μ l of cDNA, a 2 μ M concentration of RNF213 and a 10 μ M concentration of GAPDH-specific primers. The samples were separated on a 2% agarose gel stained with ethidium bromide. Cycling conditions were 15 min at 94°C, followed by 30 cycles of 30 s at 94°C, 30 s at 57°C and 30 s at 72°C. For normalization of the expression levels, we used GAPDH as an internal reference for each sample.

In situ hybridization (ISH) analysis

Paraffin-embedded blocks and sections of mouse tissues for ISH were obtained from Genostaff (Tokyo, Japan). The mouse tissues were dissected, fixed with Tissue Fixative (Genostaff), embedded in paraffin by proprietary procedures (Genostaff) and sectioned at 6 μ m. To generate anti-sense and sense RNA probes, a 521-bp DNA fragment corresponding to nucleotide positions 470–990 of mouse Rnf213 (BC038025) was subcloned into the pGEM-T Easy vector (Promega, Madison, WI, USA). Hybridization was performed with digoxigenin-labeled RNA probes at concentrations of 300 ng ml⁻¹ in Probe Diluent-1 (Genostaff) at 60°C for 16 h. Coloring reactions were performed with NBT/BCIP solution (Sigma-Aldrich, St Louis, MO, USA). The sections were counterstained with Kernechtrot stain solution (Mutoh, Tokyo, Japan), dehydrated and mounted with Malinol (Mutoh). For observation of Rnf213 expression in activated lymphocytes, 10-week-old Balb/c mice were intraperitoneally injected with 100 μ g of keyhole limpet hemocyanin and incomplete adjuvant and sacrificed in 2 weeks. The spleen of the mice was removed for Hematoxylin–eosin staining and ISH analyses.

RESULTS

Using 20 Japanese MMD families, we reevaluated the linkage mapped previously to five putative MMD loci. No locus with significant linkage, Lod score > 3.0 or NPL score > 4.0 was confirmed (Supplementary Figure 2). We conducted a genome-wide association study of 72 Japanese MMD cases. Single-marker allelic tests comparing the 72 MMD cases and 45 controls were performed for 785 720 SNPs using χ^2 statistics. These tests identified a single locus with a strong association with MMD ($P < 10^{-8}$) on chromosome 17q25-ter (Figure 1b), which is in line with the latest mapping data of a MMD locus.¹⁶ The SNP markers with $P < 10^{-6}$ are listed in Table 1. To confirm this observation, we performed a locus-specific association study. A total of 384 SNP markers (Supplementary Table 1) were selected within the chromosome 17q25-ter region and genotyped in a set of 63 MMD cases and 45 controls. The SNP markers demonstrating a high association with MMD ($P < 10^{-6}$) were clustered in a 151-kb region from base position 75 851 399–76 003 020 (SNP No.116–136 in

Table 1 A genome-wide association study of Japanese MMD patients and controls

1	SNP	Chromosome	Base position	Gene	Risk allele/ non-risk allele	Risk allele frequency in MMD	Risk allele frequency in controls	χ^2	P-value	Odds ratio	95% confidence interval	
											Lower	Upper
1	rs11870849	17	76 025 668	RNF213	T/C	0.4792	0.1111	33.55	6.95E-09	7.36	3.532	15.34
2	rs6565681	17	75 963 089	RNF213	A/G	0.7361	0.3667	31.35	2.16E-08	4.819	2.733	8.489
3	rs7216493	17	75 941 953	RNF213	G/A	0.75	0.3889	30.39	3.53E-08	4.715	2.673	8.313
4	rs7217421	17	75 850 055	RNF213	A/G	0.6667	0.3	29.86	4.64E-08	4.666	2.642	8.237
5	rs12449863	17	75 857 806	RNF213	C/T	0.6667	0.3	29.86	4.64E-08	4.666	2.642	8.237
6	rs4890009	17	75 926 103	RNF213	G/A	0.8819	0.5778	28.5	9.38E-08	5.459	2.831	10.527
7	SNP17-75933731	17	75 933 731	RNF213	G/A	0.8819	0.5778	28.5	9.38E-08	5.458	2.831	10.527
8	rs7219131	17	75 867 365	RNF213	T/C	0.6667	0.3111	28.11	1.15E-07	4.429	2.517	7.794
9	rs6565677	17	75 932 037	RNF213	T/C	0.7431	0.3977	27.43	1.63E-07	4.378	2.483	7.722
10	rs4889848	17	75 969 256	RNF213	C/T	0.75	0.4111	26.99	2.05E-07	4.297	2.444	7.889
11	rs7224239	17	75 969 771	RNF213	A/G	0.8681	0.5667	26.99	2.05E-07	5.03	2.659	9.529

Abbreviations: MMD, moyamoya disease; SNP, single-nucleotide polymorphism. A genome-wide association study testing 1,140,419 SNPs on the Human Omni-Quad 1chip (Illumina, San Diego, CA, USA) was performed in 72 Japanese MMD cases. Single-marker allelic tests between the cases and controls were performed using χ^2 statistics for all markers. This table lists the 11 SNP markers with a significance of $P < 10^{-6}$.

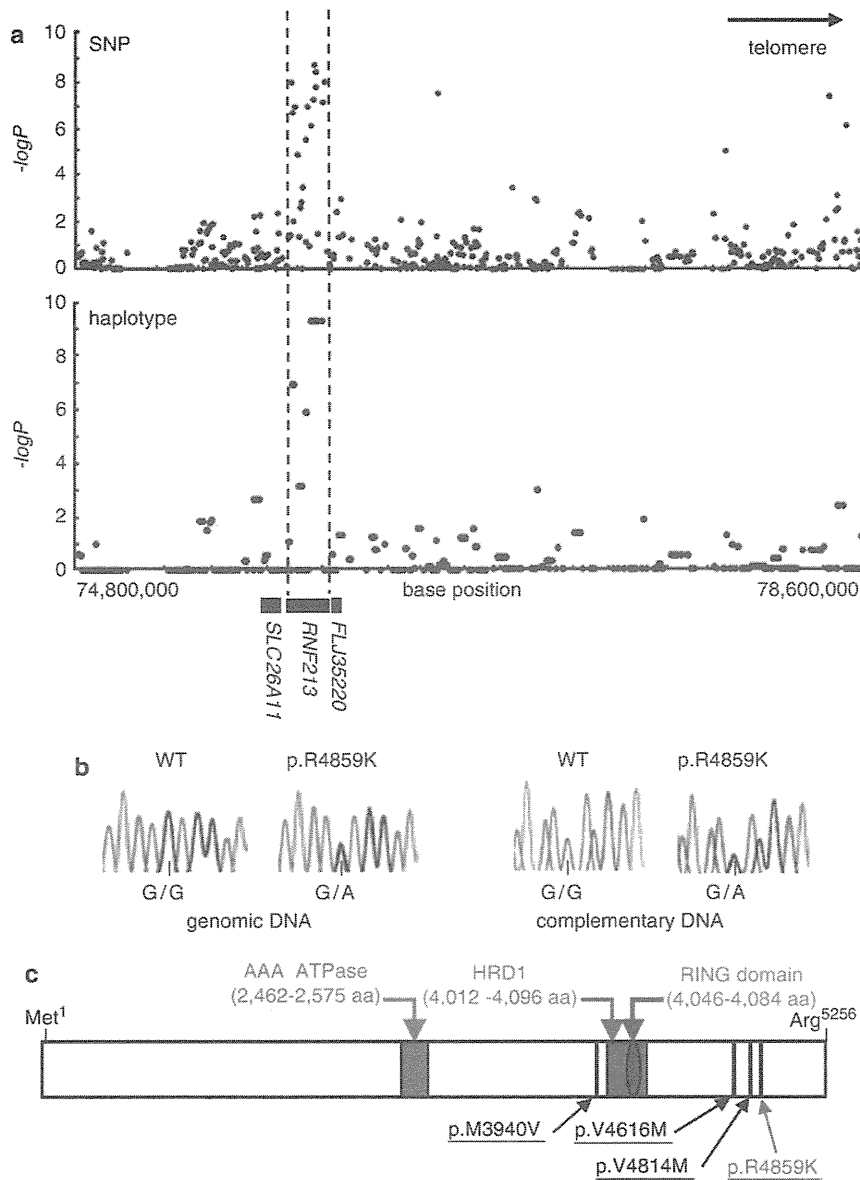


Figure 2 (a) Association analysis of 63 non-familial MMD cases and 45 control subjects. Statistical significance was evaluated by the χ^2 -test. SNP markers with a strong association with MMD ($P < 10^{-6}$) clustered in a 161-kb region (base position 75 851 399–76 012 838) indicated by two dotted lines (upper panel), which included the entire region of *RNF213* (lower panel). Haplotype analysis revealed a strong association ($P = 5.3 \times 10^{-10}$) between MMD and a single haplotype located within *RNF213*. (b) Sequencing chromatograms of the identified MMD mutations. The left panel shows the sequences of an unaffected individual and a carrier of a p.R4859K heterozygous mutation. The right panel indicates the sequencing chromatograms of the leukocyte cDNA obtained from an unaffected individual and an individual with MMD who carries the p.R4859K mutation. Note that both wild-type and mutant alleles were expressed in leukocytes. (c) The structure of the *RNF213* protein. The *RNF213* protein contains three characteristic structures, the AAA-superfamily ATPase motif, the RING motif and the HMG-CoA reductase degradation motif. The positions of four mutations identified in MMD patients are underlined, including one prevalent mutation (red) and three private mutations (black).

Supplementary Table 1); this entire region was within the *RNF213* locus (Figure 2a). A single haplotype determined by seven SNPs (SNP Nos.130–136 in Supplementary Table 1) that resided in the 3' region of *RNF213* was strongly associated with MMD onset ($P = 5.3 \times 10^{-10}$). Analysis of the linkage disequilibrium block indicated that this haplotype was not in complete linkage disequilibrium with any other haplotype in this region (Supplementary Figure 3). These results strongly suggest that a founder mutation may exist in the 3' part of *RNF213*.

Mutational analysis of the entire coding and promoter regions of *RNF213* and *FLJ35220*, a gene 3' adjacent to *RNF213*, revealed that 19 of the 20 MMD families shared the same single base substitution, c.14576G>A, in exon 60 of *RNF213* (Figure 2b and Table 2). This nucleotide change causes an amino-acid substitution from arginine⁴⁸⁵⁹ to lysine⁴⁸⁵⁹ (p.R4859K). The p.R4859K mutation was identified in 46 of 63 non-familial MMD cases (73%), including 45 heterozygotes and a single homozygote (Table 3). Both the wild-type and the p.R4859K mutant alleles were co-expressed in leukocytes

Table 2 Nucleotide changes with amino-acid substitutions identified in the sequencing analysis of *RNF213* and *FLJ35220*

Gene	Exon	Nucleotide change ^a (amino-acid substitution)	Genotype (allele)		P-value ^b	χ^2 (df=1) ^c	Odds ratio (95% CI)
			Non-familial cases	Control subjects			
<i>RNF213</i>	29	c.7809C>A (p.D2603E)	2/63 (2/126)	15/381 (15/762)	0.77	0.09	0.80 (0.2–3.6)
<i>RNF213</i>	41	c.11818A>G (p.M3940V)	1/63 (1/126)	0/388 (0/776)	0.01	6.17	ND
<i>RNF213</i>	41	c.11891A>G (p.E3964G)	4/63 (4/126)	3/55 (4/110)	0.84	0.04	1.2 (0.3–5.5)
<i>RNF213</i>	52	c.13342G>A (p.A4448T)	4/63 (4/126)	2/53 (2/106)	0.53	0.39	1.7 (0.3–9.8)
<i>RNF213</i>	56	c.13846G>A (p.V4616M)	1/63 (1/126)	0/388 (0/776)	0.01	6.17	ND
<i>RNF213</i>	59	c.14440G>A (p.V4814M)	1/63 (1/126)	0/388 (0/776)	0.01	6.17	ND
<i>RNF213</i>	60	c.14576G>A (p.R4859K)	46/63 (47/126)	6/429 (6/858)	1.2×10^{-43}	298.1	190.8 (71.7–507.9)
<i>FLJ35220</i>		None					

Abbreviations: ND, not determined; SNP, single-nucleotide polymorphism.

^aNucleotide numbers of *RNF213* cDNA are counted from the A of the ATG initiator methionine codon (NCBI Reference sequence, NP_065965.4).

^bP-values were calculated by Fisher's exact test.

^cGenotypic distribution (carrier of the polymorphism vs non-carrier).

Table 3 Association of the p.R4859K (c.14576G>A) mutation with MMD

	Total	Genotype		
		wt/wt (%)	wt/p.R4859K (%)	p.R4859K/p.R4859K (%) ^d
<i>Members of 19 MMD families^a</i>				
Affected	42	0	39 (92.9)	3 (7.1)
Not affected	28	15 (53.6)	13 (46.4)	0
<i>Individuals without a family history of MMD^{b,c}</i>				
Affected	63	17 (27.0)	45 (71.4)	1 (1.6)
Not affected	429	423 (98.6)	6 (1.4)	0

Abbreviations: MMD, moyamoya disease.

^aEntire distribution, $\chi^2=29.4$, $P=4.2 \times 10^{-7}$.

^bEntire distribution, $\chi^2=298.2$, $P=1.8 \times 10^{-65}$.

^cGenotypic distribution (p.R4859K carrier vs non-carrier), $\chi^2=298.1$, $P=1.2 \times 10^{-43}$, odds ratio=190.8 (95% CI=71.7–507.9).

^dThe age of onset and initial symptoms of the four homozygotes were comparable to those of the 84 heterozygous patients.

in three patients heterozygous for the p.R4859K mutation (Figure 2b), excluding the possible instability of the mutant *RNF213* mRNA. Additional missense mutations, p.M3940V, p.V4616M and p.V4814M, were detected in three non-familial MMD cases without the p.R4859K mutation (Figure 2c). These mutations were not found in 388 control subjects and were detected in only one patient, suggesting that they were private mutations (Table 2). No copy number variation or mutation was identified in the *RNF213* locus of 12 MMD patients using comparative genome hybridization microarray analysis (Supplementary Figure 4). In total, 6 of the 429 control subjects (1.4%) were found to be heterozygous carriers of p.R4859K. Therefore, we concluded that the p.R4859K mutation increases the risk of MMD by a remarkably high amount (odds ratio=190.8 (95% confidence interval=71.7–507.9), $P=1.2 \times 10^{-43}$) (Table 3). It was recently reported that an SNP (ss161110142) in the promoter region of *RPTOR*, which is located ~150 kb downstream from *RNF213*, was associated with MMD.¹⁷ Genotyping of the SNP in *RPTOR* showed that the *RNF213* p.R4859K mutation was more strongly associated with MMD than ss161110142 (Supplementary Figure 1).

RNF213 encodes a protein with 5256 amino acids harboring a RING (really interesting new gene) finger motif, suggesting that it

functions as an E3 ubiquitin ligase (Figure 2c). It also has an AAA ATPase domain, which is characteristic of energy-dependent unfoldases.¹⁸ To our knowledge, *RNF213* is the first RING finger protein known to contain an AAA ATPase domain. The expression profile of *RNF213* has not been previously fully characterized. We performed a quantitative reverse transcription PCR analysis in various human tissues and cells. *RNF213* mRNA was highly expressed in immune tissues, such as spleen and leukocytes (Figure 3a and Supplementary Figure 5). Expression of *RNF213* was detected in fractions of both polymorphonuclear cells and mononuclear cells and was found in both B and T cell fractions (Supplementary Figure 6). A low but significant expression of *RNF213* was also observed in human umbilical vein endothelial cells and human pulmonary artery smooth muscle cells. Cellular expression was not enhanced in tumor cell lines, compared with leukocytes. In human fetal tissues, the highest expression was observed in leukocytes and the thymus (Supplementary Figure 6E). The expression of *RNF213* was surprisingly low in both adult and fetal brains. Overall, *RNF213* was ubiquitously expressed, and the highest expression was observed in immune tissues.

We studied the cellular expression of *Rnf213* in mice. The ISH analysis of spleen showed that *Rnf213* mRNA was present in small mononuclear cells, which were mainly localized in the white pulps (Figures 3b–g). The ISH signals were also detected in the primary follicles in the lymph node and in thymocytes in the medulla of the thymus (Supplementary Figure 7). To study *Rnf213* expression in activated lymphocytes we immunized mice with keyhole limpet hemocyanin, and examined *Rnf213* mRNA in spleen by ISH analysis. Primary immunization with keyhole limpet hemocyanin antigen revealed that the expression of *Rnf213* in the secondary follicle is as high as in the primary follicle in the lymph node (Supplementary Figure 8). In an E16.5 mouse embryo, expression was observed in the medulla of the thymus and in the cells around the mucous palatine glands (Supplementary Figure 9). These findings suggest that mature lymphocytes in a static state express *Rnf213* mRNA at a higher level than do their immature counterparts.

DISCUSSION

We identified a susceptibility locus for MMD by genome-wide and locus-specific association studies. Further sequencing analysis revealed a founder missense mutation in *RNF213*, p.R4859K, which was tightly associated with MMD onset. Identification of a founder mutation in individuals with MMD would resolve the following recurrent